SPATIOTEMPORAL VARIATIONS OF ATMOSPHERIC BLACK CARBON CONCENTRATIONS IN KOLKATA & HOWRAH MUNICIPAL CORPORATION AREAS

WEST BENGAL

teri THE ENERGY AND RESOURCES INSTITUTE
Creating Innovative Solutions for a Sustainable Future

SPATIOTEMPORAL VARIATIONS OF ATMOSPHERIC BLACK CARBON CONCENTRATIONS IN KOLKATA & HOWRAH MUNICIPAL CORPORATION AREAS

Prepared for

West Bengal Pollution Control Board

teri THE ENERGY AND RESOURCES INSTITUTE
Creating Innovative Solutions for a Sustainable Future

TERI, 2025

Project Advisors, The Energy and Resources Institute (TERI)
Dr Prodipto Ghosh
Dr Syamal Kumar Sarkar

Project Team, The Energy and Resources Institute (TERI)
Dr Arindam Datta
Md Hafizur Rahman
Mr Suresh Ramasubramanya Iyer
Mr Nimish Singh
Mr Prabhat Sharma
Mr Justin Jacob
Mr Dheeraj Mehra
Mr Ved Prakash Sharma
Ms Shivani Sharma
Mr Runkob Srimani
Ms Laboni Pal
Ms Purbasha Das
Mr Shaheen Hassan Dhawan

Field Team
Mr Surinder Singh Negi
Mr Kulwant Singh
Mr Virender Vaid
Mr Mahesh Kumar
Late Mr K Johnson

Editorial Team
Sachin Bhardwaj
Rajiv Sharma
Vijay Nipane

University of Calcutta (Local Knowledge Partner)
Dr Punarbasu Chaudhuri

Future Institute of Technology (Local Knowledge Partner)
Dr Pradipta K Banerjee
Akash Halder
Soumya Panja
Sulagna Karmakar

For more information

Project Monitoring Cell
The Energy and Resources Institute (T E R I)
Core 6C, IHC Complex
Lodhi Road
New Delhi – 110 003
India

Tel. 2468 2100 or 2468 2111
E-mail pmc@teri.res.in
Fax 2468 2144 or 2468 2145
Web www.teriin.org
India +91, Delhi (0)11

Contents

List of **Tables**

List of **Figures**

Background

Atmospheric black carbon (BC) is one of the short-lived climate pollutants (SLCPs) contributing to climate change. It warms the Earth by absorbing sunlight, heating the atmosphere by reducing albedo when deposited on snow and ice (direct effects), and indirectly by interaction with clouds, with a total forcing of 1.1 W/m^2. The BC has a warming impact on climate that is 460-1,500 times stronger than CO_2 per unit of mass. However, it can stay in the atmosphere for only a few days to weeks, compared to 300 to 1000 years of atmospheric lifetime of CO_2. On the other hand, the atmospheric BC is part of $PM_{2.5}$ as per the aerodynamic diameter of the particle. Thus, atmospheric BC is not only important from the health point of view, but reduction of atmospheric BC emission can have an immediate effect on climate change considering its shorter lifetime.

BC is emitted from the incomplete combustion of fossil fuel, biomass, solid waste, etc. (Zhang *et al.*, 2021). Biomass burning and fossil fuel burning contribute nearly 80% of the total global BC (Jing *et al.*, 2019). In addition, transport (~28%) and residential fuel combustion (~58%) are also the major contributors to global BC emissions from fossil fuels while on the regional scale, their contribution to atmospheric BC emission changes drastically (Klimont *et al.* 2017). The major sources of BC particles in urban locations are vehicle exhaust, industries, thermal power plants, and biomass for residential fuel use.

The Indo-Gangetic Plain (IGP) is one of the largest populated and polluted river basins in the world experiencing higher aerosol loading (including BC) throughout the year in association with strong intra-seasonal to inter-annual variation (Rana *et al.*, 2023). Located in the eastern part of the IGP outflow region and close to the land-ocean boundary, Kolkata and Howrah are susceptible to contrasting seasonal maritime airflow from the Bay of Bengal and continental air mass from the IGP and Himalayan region, which regulates the local concentration of BC. The distinctive presence of pre-monsoon, monsoon, and winter seasons in Kolkata and Howrah also makes it important to study the control of meteorological parameters on the variation of BC loading in the atmosphere.

Studies reported prominent seasonal and diurnal variations in atmospheric BC concentration associated with the meteorological parameters in Kolkata. Talukdar *et al.* (2015) examined near-surface aerosol BC concentration collected using a seven-channel aethalometer (AE31) from June 2012–May 2013 in Kolkata. The study reported mean BC concentration varying between 5 $\mu g/m^3$ and 27 $\mu g/m^3$ seasonally. Atmospheric boundary layer dynamics and seasonal variation of mass transportation significantly influence BC concentration. An estimation of the Angstrom exponent revealed fossil fuel combustion as a major source of BC in Kolkata. The atmospheric concentration of BC showed two maximum events daily, one during the morning and another in the evening. However, an unusual pattern was observed following the rain events. During normal days, BC

concentrations remained around 8 μg /m^3 in the noon and early afternoon, but surprisingly after thunderstorms, they unexpectedly rose over to 20 μg /m^3 (Talukdar *et al.*, 2014). This increase was linked to the formation of local temperature inversions after rain, which suppresses vertical mixing and dispersion of BC, unlike on non-rainy days.

Verma *et al.* (2013) assessed BC concentrations, its radiative effects, and sources in Kolkata during the winter season using ground-based measurements and modelling tools. BC concentrations exhibited higher variability during the evening to early morning hours compared to daytime. The recorded average BC surface mass concentration was 11 μg/m^3, contributing 3–10% to total aerosol mass and 9–16% to submicronic aerosols. The BC optical depth (AOD) was 0.11, with BC accounting for 13% of the total AOD. The study reported that the radiative forcing due to BC at the top of the atmosphere was +0.94 W/m^3, which is 59% of the total global radiative forcing resulting from carbon dioxide. Moreover, modelling output showed that BC in East India is mainly from biofuel and fossil fuel combustion, with the IGP contributing significantly. However, long-range transport from biomass burning outside the IGP also plays a key role in BC columnar loading.

Rana *et al.* (2020) measured aerosol BC and aqueous and methanol-extractable brown carbon from a receptor location under two aerosol regimes: the photochemistry-dominated summer and biomass-burning-dominated post-monsoon. They reported a BC concentration of ~1.7–25.3 μg/m^3 with an average value of 12.1 ± 5.7 μg/m^3 during the post-monsoon season in the metropolitan city of Kolkata. However, in the biomass-burning regime, both BC and its biomass-burning-derived fraction increased by factors of 3–4 over the summertime values and brown carbon absorption coefficients also rose significantly during biomass burning.

Using updated BC emission inventories, Ghosh *et al.* (2020) investigated the direct radiative changes due to the atmospheric BC concentration during the winter months using an effectively simulated BC distribution over the IGP employing a high-resolution (0.1° × 0.1°) chemical transport model, CHIMERE. Estimated mean daily atmospheric BC concentrations (33 μg/m^3) and aerosol optical depth (AOD) were higher in Kolkata compared to other locations in the IGP. Additionally, the radiative warming of the atmosphere (30 W/m^2 to +50 W/m^2) was estimated to be about 50%–70% larger than the cooling due to BC at the surface.

Wind flow from the IGP contributes to anomalous atmospheric BC concentration in Kolkata and Howrah cities, especially increasing the concentration during weekends and holidays when local emissions are low (Rakshit *et al.*, 2023). High BC events were associated with enhanced atmospheric heating below the boundary layer (2000 m) and negative surface radiative forcing.

The mean BC concentration in Kolkata was 12.6 ± 6.8 μg/m^3 attributing to the combined effects of the prevailing urbanization and meteorology assessing the diurnal, seasonal, and long-term BC trends at multisite IMD stations during the period 2016–21 (Kumar *et al.*, 2023).

This suggests that there are significantly higher concentrations of atmospheric BC in Kolkata and surrounding areas compared to other locations in the IGP vis-vis there are a substantial number of

sources of atmospheric BC in Kolkata and Howrah. However, there is no systematic spatiotemporal study of BC in the area which could help to develop policy measures to manage the emissions of BC from Kolkata and the surrounding areas.

The Kolkata and Howrah cites

Kolkata and Howrah cities are in the southern part of West Bengal (Figure 1). Kolkata city is on the eastern flank of Hooghly River and Howrah city is on the western side. Kolkata city covers the entire district of Kolkata and Howrah city is in the north-eastern side of Howrah district of the state. A blend of historical significance, cultural richness, and economic importance makes both cities unique and vibrant.

The archaeologists believe that the region covering the city of Kolkata has been inhabited for over 2,000 years, but its documented history begins with the arrival of the British East India Company in 1690. On the other hand, the history of Howrah city is more than 500 years old. The East India Company played a major role in the development of both cities. Kolkata (erstwhile Calcutta) was the capital of British India. The first riverine port was established in this city by the British. Many factories were built in Howrah by the British. This is the reason Howrah was known as the 'Sheffield

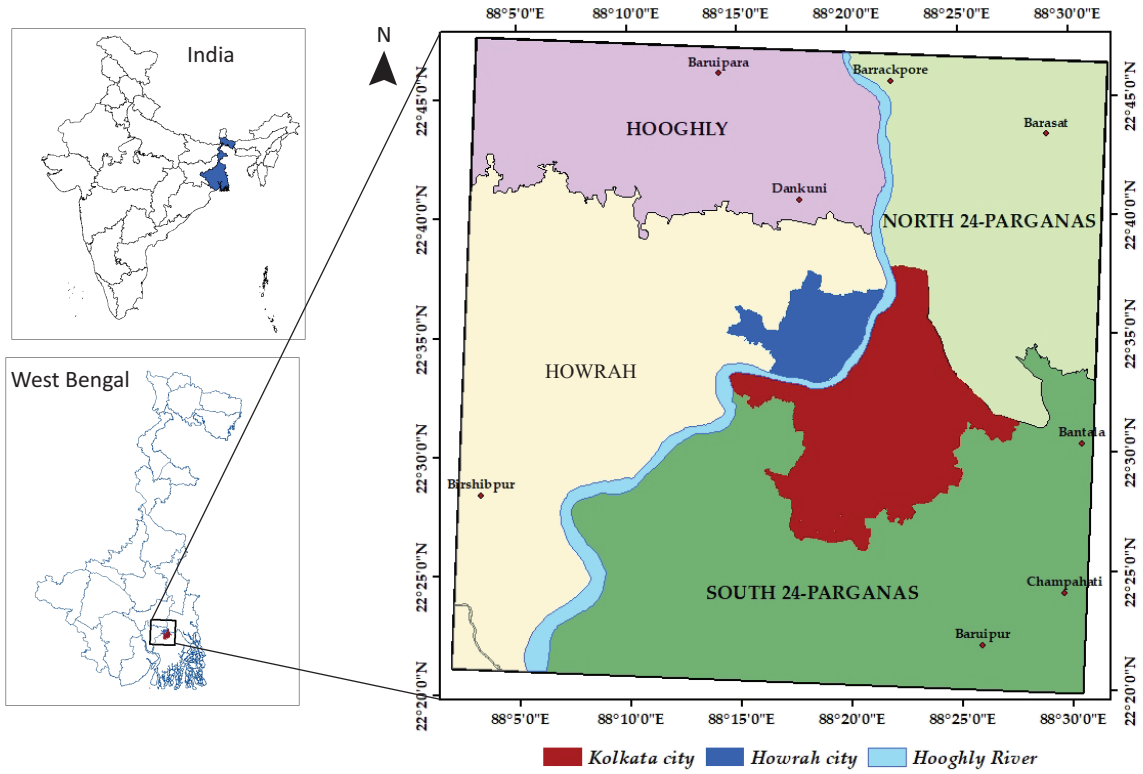

FIGURE 1 Location of Kolkata and Howrah cities

of the East'. Eventually, it also emerged as the major transport hub in eastern India. Howrah is also known as the 'Glasgow of India', following its similarities with the industrial city of Glasgow in Scotland. Kolkata is popular as a 'city of joy', following its rich culture, history, literature, and enthusiasm for life. Kolkata is the capital of West Bengal. It is the principal commercial, cultural, and educational centre of East India. The famous Howrah Bridge (Rabindra Setu) over Hooghly River, connects both the cities since 1943. At present, there are two bridges (Rabindra Setu and Vidyasagar Setu) over the Hooghly River to connect the twin cities of Kolkata and Howrah.

The beginning of industrial growth in Kolkata and the adjacent areas dates to British colonial authority in the 19th century. Many enterprises were established because of this ideal location, including shipbuilding yards, cotton mills, and jute mills. The abundance of raw resources from the hinterlands and the city's well-developed transit system drove the early industrial boom. The primary port for the transshipment of cotton and indigo to Europe was Kolkata. During the post-colonial era, state-led initiatives led to a concentration on heavy industrial sectors like steel and engineering. In addition, many banks and businesses built their headquarters in Kolkata because it served as the capital of British India.

Following a well-established centre of industry, culture, and trade, Kolkata and adjacent areas draw immigrants from all over India and beyond. Migrants looking for improved living circumstances and economic possibilities were drawn to the area from Bihar, Odisha, eastern Uttar Pradesh, and the western part of the country. The long history of urbanization and immigration makes both cities and the region one of the most congested and densely populated areas in India. Kolkata and Howrah are, respectively, the third and fourth most densely populated (approximately 24,000 people/sq. km and 16,000 people/sq. km, respectively) cities in India after Mumbai and Chennai.

Kolkata Municipal Corporation

Kolkata Municipal Corporation (KMC), established in 1876, is the governing body responsible for the civic infrastructure and administration of the city of Kolkata. The KMC is the third-oldest municipal corporation in India after Chennai and Mumbai. The KMC is divided into administrative units called boroughs and wards. The KMC has the largest municipal corporation area (206 sq. km) in West Bengal. At present, there are 144 wards in KMC distributed in 16 Boroughs (Figure 2).

The main functions of KMC include water supply, waste management, road maintenance, public health, and sanitation. There are 144 Urban Primary Health Centres (UPHCs) under the KMC. The areas of KMC and Kolkata Police are coterminous. Sealdah Railway Station in Kolkata is one of the important railway stations in India. After Howrah Railway Station, it is the second-largest railway station in India. About 1.5 million commuters pass through the station every day.

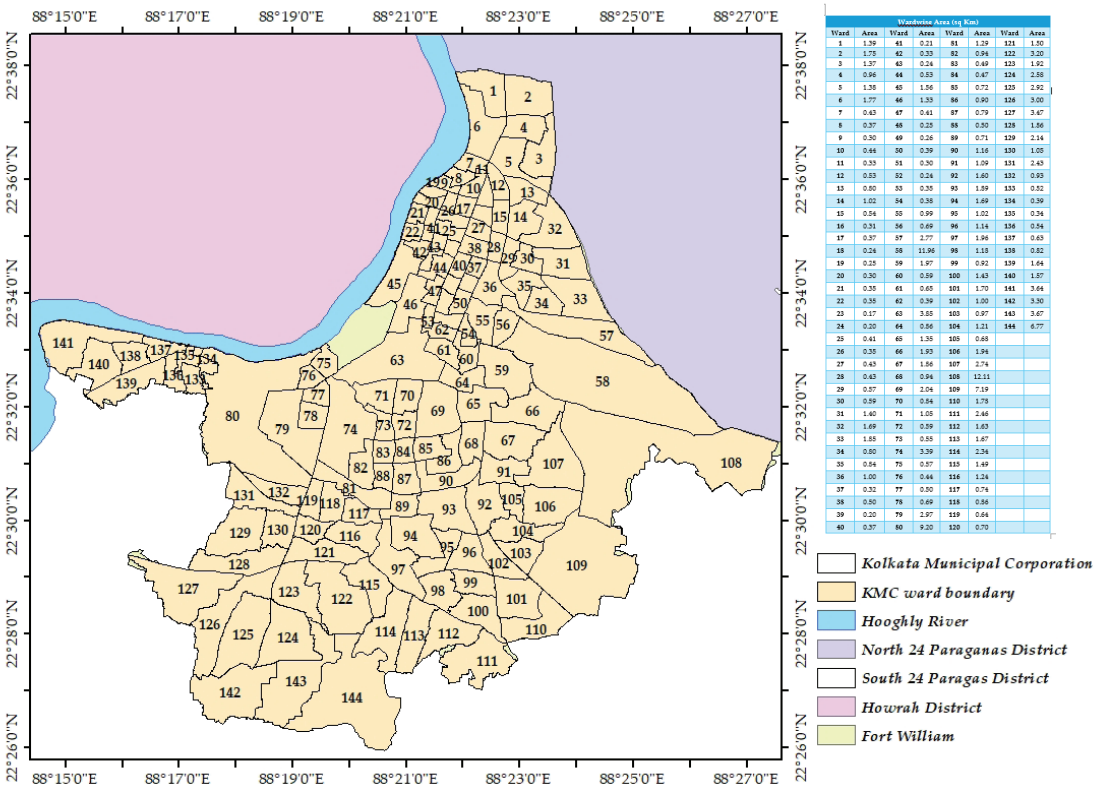

Wardwise Area (sq Km)

Ward	Area	Ward	Area	Ward	Area	Ward	Area
1	1.29	41	0.21	81	1.29	121	1.50
2	1.75	42	0.33	82	0.94	122	3.20
3	1.37	43	0.24	83	0.49	123	1.92
4	0.96	44	0.53	84	0.47	124	2.58
5	1.36	45	1.56	85	0.72	125	2.91
6	1.77	46	1.33	86	0.90	126	3.00
7	0.43	47	0.41	87	0.79	127	3.47
8	0.37	48	0.25	88	0.80	128	1.86
9	0.30	49	0.26	89	0.71	129	2.14
10	0.44	50	0.39	90	1.16	130	1.05
11	0.33	51	0.30	91	1.09	131	2.43
12	0.53	52	0.24	92	1.60	132	0.93
13	0.80	53	0.35	93	1.89	133	0.82
14	1.02	54	0.38	94	1.69	134	0.39
15	0.54	55	0.99	95	1.02	135	0.34
16	0.31	56	0.69	96	1.14	136	0.54
17	0.37	57	2.77	97	1.96	137	0.65
18	0.24	58	11.96	98	1.18	138	0.82
19	0.25	59	1.97	99	0.92	139	1.64
20	0.30	60	0.59	100	1.43	140	1.57
21	0.35	61	0.65	101	1.70	141	3.64
22	0.35	62	0.39	102	1.00	142	3.30
23	0.17	63	3.85	103	0.97	143	3.67
24	0.20	64	0.86	104	1.21	144	6.77
25	0.41	65	1.35	105	0.65		
26	0.25	66	1.93	106	1.94		
27	0.43	67	1.86	107	2.74		
28	0.43	68	0.94	108	12.11		
29	0.87	69	2.04	109	7.19		
30	0.59	70	0.84	110	1.78		
31	1.40	71	1.05	111	2.46		
32	1.69	72	0.59	112	1.63		
33	1.85	73	0.55	113	1.67		
34	0.80	74	3.39	114	2.34		
35	0.84	75	0.87	115	1.49		
36	1.00	76	0.44	116	1.24		
37	0.32	77	0.50	117	0.74		
38	0.50	78	0.69	118	0.86		
39	0.20	79	2.97	119	0.64		
40	0.37	80	9.20	120	0.70		

FIGURE 2 The Kolkata Municipal Corporation area

Howrah Municipal Corporation

Howrah City is presently governed by the Howrah Municipal Corporation (HMC) which was established in 1980. It is worth mentioning, the Howrah municipality was established in 1864 after the establishment of Howrah Railway Station. Later, the Bally municipality was merged with Howrah municipality to form the HMC. In the year 2021, Bally municipality was separated from the HMC area as a separate municipality. At present, HMC is the second-largest municipal corporation in West Bengal with about 63.5 sq. km area distributed in 50 wards (Figure 3). There are seven boroughs under the HMC. Fifteen UPHCs are presently functional under the HMC. The Howrah Railway Station is the oldest as well as the largest and busiest railway station in India.

Description of the study

The West Bengal Pollution Control Board (WBPCB) invited The Energy and Resources Institute (TERI), New Delhi, to submit a proposal to analyze the spatiotemporal variations in atmospheric BC in Kolkata and Howrah cities. Accordingly, TERI submitted a technical and financial proposal to WBPCB to prepare an annual spatiotemporal variation of atmospheric BC concentration

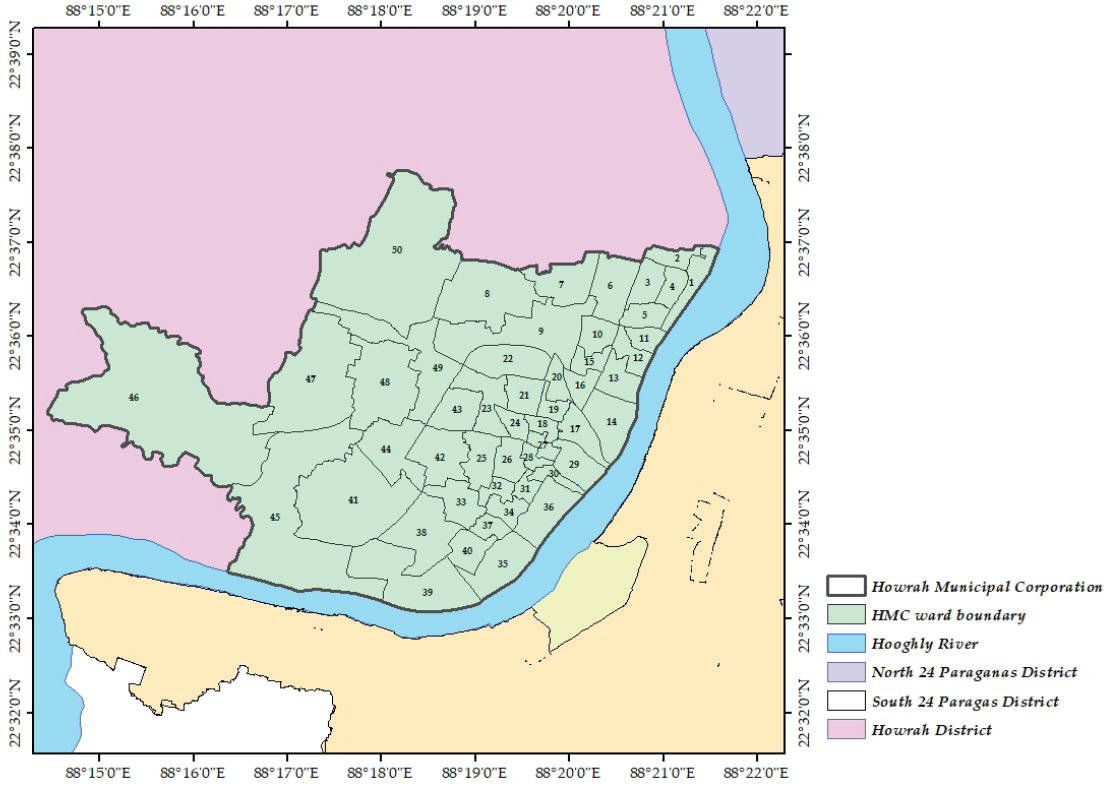

FIGURE 3 The Howrah Municipal Corporation area

over Kolkata and Howrah in March 2023. Following the review of the proposal by experts, WBPCB awarded the project to TERI on 10th May 2023 (Memo No. 1139/1K-1/2021). Under the memorandum of understanding (MoU) signed (e-stamp Certificate No. lN-Dt_93620208110842U) between the WBPCB and TERI in May 2023. The objectives of the projects are,

» Spatiotemporal variation of atmospheric BC concentration in KMC and HMC areas during the winter period.

» Spatiotemporal variation of atmospheric BC concentration in KMC and HMC areas during the summer period.

» Sectorial emission inventory of BC in KMC and HMC areas.

This report is divided into three chapters: I. Measurement of atmospheric BC in Kolkata and Howrah, II. Sectoral emission inventory of atmospheric BC in Kolkata and Howrah, and III. Spatial variation of atmospheric BC concentrations in Kolkata and Howrah. The sectoral activity data estimated from the survey conducted during the air pollution source apportionment and atmospheric carrying capacity study in Kolkata and Howrah was used to built the sectorial emission inventory of BC.

Measurement of Atmospheric Black Carbon

The study area has a tropical savanna climate. The weather is generally characterized by three prominent seasons: summer (March to June), monsoon (July to September), and winter (November to February). The average annual temperature in the area is about 26°C with a precipitation of about 1800 mm of which more than 80% is received during the SW monsoon (JJAS). Relative humidity in the area varies between 51% to 95% during different seasons. The summer temperature in KMC and the HMC area ranges between 29°C and 45°C. May is usually the hottest month, with temperatures frequently reaching more than 40°C. Despite the heat, pre-monsoon showers, thunderstorms, and hailstorms, known locally as 'Kalbaishakhi', also occur during the summer season. Deep depression and cyclones are common during the end of the monsoon season. Winter in the KMC and the HMC area is mild and comfortable, with ambient temperatures ranging from 8°C to 25°C.

The air quality was measured during the summer and winter seasons. The wind pattern in the area significantly changes during each season. In summer, the major wind is southerly, while it is northerly and northwesterly during winter (Figure 4).

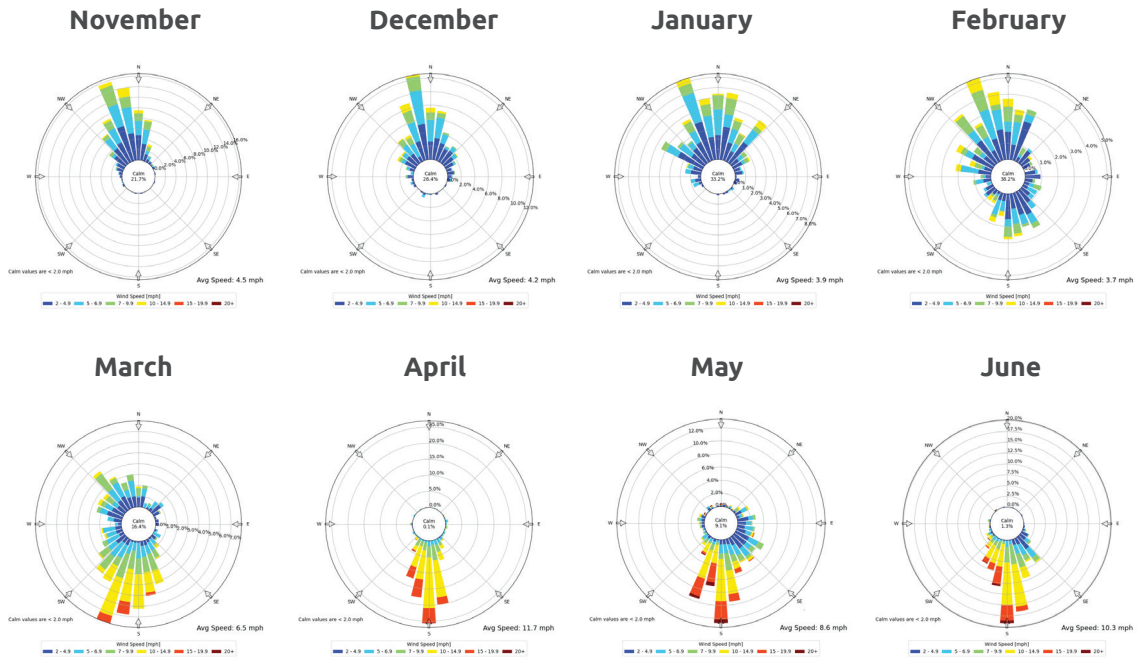

FIGURE 4 Monthly windrose of the area during winter (top) and summer (bottom) seasons

Air quality measurement locations in both cities were selected following the Central Pollution Control Board (CPCB) guidelines (CPCB, 2019). Six air quality measurement locations were selected in the KMC area and four in the HMC area. Air quality measurement locations were selected based on the land use type in each city – i) residential, ii) commercial, iii) industrial, and iv) kerbside. Background location was selected with respect to each city based on the seasonal predominant wind direction in the area (Figure 4). Thirty areas covering different land-use types were initially shortlisted following recce in both cities as probable air quality measurement locations based on the land-use type. Following discussions with the experts of the WBPCB, KMC, and HMC, six locations were selected in the KMC area, and four locations were selected in the HMC area from the shortlisted areas. Summer and winter seasons background air quality measurement locations were also selected in consultation with experts.

After checking the feasibility of installing and operating the air quality measurement instruments, 14 locations of air quality measurement (Table 1) were finalized at the selected areas that were finalized in discussion with the experts.

All selected air quality measurement locations were spatially covered in each city (Figure 5).

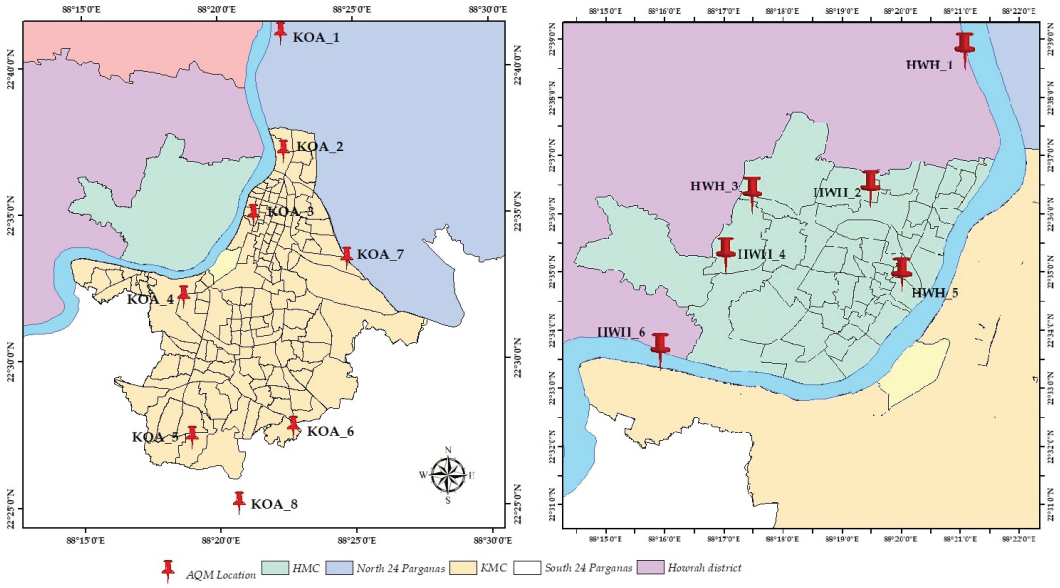

FIGURE 5 Spatial distribution of air quality measurement (AQM) locations in the KMC and HMC area

TABLE 1 Description of selected air quality measurement locations

Location ID	Location	Land-use	Description
KMC area			
KOA_1	Panihati	Background (Winter)	The area, surrounded by residential households, is within the Barrackpore industrial area, with major industries like Bengal Chemical & Pharmaceutical Ltd, Texmaco Rail & Engineering Ltd, and Tractor India Ltd nearby.
KOA_2	Cossipore	Commercial	Major commercial hub of cement in West Bengal and eastern India.
KOA_3	Boro Bazar	Commercial	One of the largest wholesale markets in the country, located near to the Howrah and Sealdah stations.
KOA_4	Khidderpur	Industrial	It is the largest riverine port (Shyama Prasad Mukherjee Port) in India. The location is near to coal-handling area of the port. Southern Thermal Power Station is near to the location. Slum areas is near to the location.
KOA_5	Thakurpukur	Residential	Surrounded with residential households. Construction activities, slum areas and occasional burning of refuse materials are evident near the location.
KOA_6	Garia	Residential	A typical residential area. A major bus terminus, playground and crematorium nearby.
KOA_7	Chingrighata	Kerbside	A major traffic junction on the EM bypass. East Kolkata wetland is nearby. A canal and slum area in the vicinity.
KOA_8	Raghavpur	Background (Summer)	The location was in the middle of greenery. Agriculture fields, plantation areas, fishponds, playgrounds and rural residential households are present near the location.
HMC area			
HWH_1	Bally	Background (Winter)	Located on the western flank of the Hooghly River near the Nivedita Setu (NH-12) and G T Road.
HWH_2	Belgachia	Industrial	A large number of coal and biomass-using industries, major municipal solid waste dump sites of HMC, and medical waste incineration units are near the location. Mostly slum households surround the location.
HWH_3	Balitikuri	Residential	Surrounded by urban households. The biomass material industry is nearby.
HWH_4	Jagacha	Kerbside	Located near Kona Expressway. The location is surrounded by residential households.
HWH_5	Howrah Maidan	Commercial	Major wholesale markets, offices, district hospital, and district court are near the location alongside major bus terminus.
HWH_6	Podra	Background (Summer)	At the river line. The location is near Hooghly Cochin Shipyard Ltd.

Measurement of Atmospheric BC Concentrations

Atmospheric concentrations of BC were measured at all selected AQM locations during the winter and summer seasons. Atmospheric BC concentrations were measured at 4 to 8 m height from ground level at each AQM location (i.e. about the height of a single-storey building) (Figure 6, Figure 7).

FIGURE 6 Atmospheric pollution measurement at selected AQM locations in the KMC area and the background station

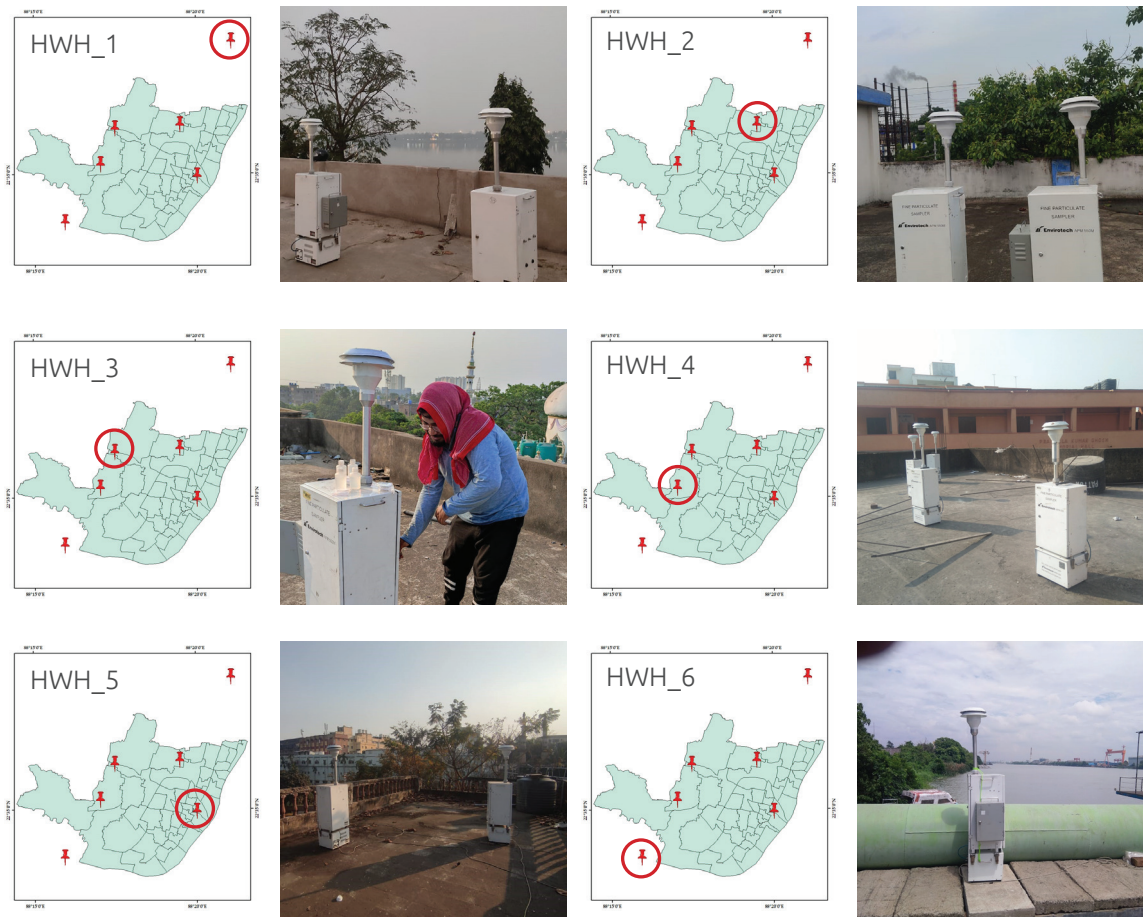

FIGURE 7 Atmospheric pollution measurement at selected AQM locations in the HMC area and the background station

Atmospheric $PM_{2.5}$ samples were collected from different AQM locations during December 2022 and January 2023 (Winter season – W1), between April 2023 and May 2023 (summer season - S). The winter season atmospheric $PM_{2.5}$ samples were collected again in December 2023 and January 2024 (W2) to study the consistency of atmospheric BC concentration in the area. At each of the AQM locations, a 24-hour air quality measurement was carried out for 15 continuous days in each season. Atmospheric $PM_{2.5}$ concentrations were measured following the gravimetric method using APM 550 fine particulate samplers (Envirotech, New Delhi). The flow rate of the air sample was maintained at 16.7 litres per minute (LPM). The flow gauge of the fine particulate samplers was calibrated, and the particulate matter impactor was cleaned before the start of the air quality measurement. A flow calibrator was used to check the airflow of the fine particulate samplers at regular intervals. $PM_{2.5}$ samples were collected on Quartz filter media for the measurement of the BC.

A multi-wavelength thermal/optical EC/OC Carbon Analyser (DRI Model 2015 Series 2; Mars Bioanalytical Pvt. Ltd) was used to measure the EC in the $PM_{2.5}$ samples collected on quartz filter media. It utilizes a thermal-optical analysis technique to quantify the amount of carbon by heating the sample and measuring the optical properties of the emitted gases. The instrument also measures transmission (T) intensities as light attenuation (ATN_Y) at multiple wavelengths (405, 445, 532, 635, 780, 808, and 980 nm).

The filter-loading adjustment on ATN_Y for multiwavelength thermal/optical carbon analysis attenuation is empirically derived according to the ATN_Y-EC correspondence. Samples were classified into 14 ranges with increments of 1 to 5 µg/cm^2 of EC filter loadings or 0.107 to 0.53 µg/m^3 EC concentration.

EC loadings were expressed as aerial densities (µg/cm^2) (***Annexure I***) so that results can be extrapolated to different deposit areas. The response of ATN_Y to the EC loading diminishes with increased EC loading. ATN_Y at each wavelength is then adjusted upward assuming the response should be the same as at lower filter loadings. The adjusted attenuation was then apportioned into BrC and BC.

The corrected ATN_Y is linearly related to EC loading and, generally, the EC light absorption coefficient. Since aerosol absorption decreases exponentially with increasing wavelength, the Absorption Ångström Exponent (AAE) of pure BC or BrC can be estimated by ***eq. 1*** fitting all seven wavelengths with the derived coefficient (Annexure I).

$$ATN_Y = C \times Y^{-AAE} \qquad \textit{eq.1}$$

while for a BC-BrC mixture, ATN_Y can be further separated based on ***eq. 2***

$$ATN_Y = ATN(BC)_Y + ATN(BrC)_Y \qquad \textit{eq.2}$$

where, $ATN(BC)_Y = q(BC) \times Y^{-AAE(BC)}$ and $ATN(BrC)_Y = q(BrC) \times Y^{-AAE(BrC)}$

Assuming that BrC contributes negligibly to light absorption at $Y \geq 635$ nm (Andrae and Glencser, 2006), AAE_{BC} was calculated based on adjusted wavelength at 635 nm, 780 nm, 808 nm and 980 nm.

Thus the BrC concentration in each filter was calculated using the adjusted ATN405, ATN445, and ATN532

The volume of air sampled was used to calculate the BC and BrC concentrations in µg/m^3.

Atmospheric black carbon concentrations in the Kolkata Municipal Corporation area

Daily variations in the atmospheric BC concentrations at different AQM locations during the measurement period were much higher during the winter season compared to the summer season (Figure 8).

During the summer season, the atmospheric concentration of BC varied between 2 μg/m^3 and 8 μg/m^3(Figure 8). The mean atmospheric concentration of BC in the KMC area during the summer season was measured as 5 μg/m^3. During the winter season, the atmospheric concentrations of BC varied between 1 μg/m^3 and 21 μg/m^3 during W1 and 6 μg/m^3 and 17 μg/m^3 during W2 among the AQM locations. Mean atmospheric concentrations of BC during the W1 and W2 periods in the KMC area were measured as 12 μg/m^3 and 11 μg/m^3, respectively (Figure 8). Among different locations in the KMC area, the highest atmospheric BC concentration was measured at KOA_4 during the W1 period and at KOA_7 during the W2 period. The usage of fuelwood and coal in the residential cooking at the slum areas near KOA_4 and KOA_7 might have been attributed to the highest concentrations of atmospheric BC at these locations. Additionally, the large-scale movement of vehicles at these locations might also have been attributed to the atmospheric BC concentrations.

The variations in the atmospheric BrC concentrations at different AQM locations during the measurement period were also higher during the winter season compared to the summer season. During the measurement period, the highest atmospheric BC concentration (20 μg/m^3) was recorded at the KOA_4 location during the W1 period (Figure 8). Among different AQM, the mean atmospheric BrC concentration (8 μg/m^3) was also recorded as the highest at the KOA_4 location during the W1 period (Figure 8).

During summer and W2 there was no significant difference ($P>0.05$) in atmospheric BC concentrations at different AQM locations in the KMC area. Mean atmospheric BC concentration was significantly ($P < 0.05$) higher at KOA_4 (16 μg/m^3) followed by KOA_6 and KOA_7 (Table 2). Study also suggests that there was no significant difference in the atmospheric BC concentrations among W1 and W2 (Table 2).

Atmospheric black carbon concentrations in the Howrah Municipal Corporation area

Daily variations in the atmospheric BC concentrations at different AQM locations in the HMC area during the measurement period were much higher during the winter season compared to the summer season. Atmospheric BrC concentrations at different AQM locations were also recorded lower during the summer season compared to the winter (Figure 9).

During the W1 season, the daily atmospheric BC concentrations varied between 5 μg/m^3 and 17 μg/m^3 while it varied between 1 μg/m^3 and 15 μg/m^3 during the W2 season (Figure 9). The largest daily variation of atmospheric BC concentration was recorded during the W2 season compared to the other two seasons. During the summer season, the daily atmospheric concentration of BC varied between 1 μg/m^3 and 8 μg/m^3 at the AQM locations in the HMC area (Figure 9). Among different locations in the HMC area, the highest atmospheric BC concentration was measured at HWH_3 (18 μg/m^3) during the W1 period. During the summer season, the highest atmospheric BC concentration was measured at HWH_4 (7 μg/m^3), and during the W2 period highest atmospheric BC concentration was measured at HWH_5 (15 μg/m^3). Emissions from the vehicular tailpipe might have attributed to the higher atmospheric BC concentrations at HWH_4 and HWH_5, however,

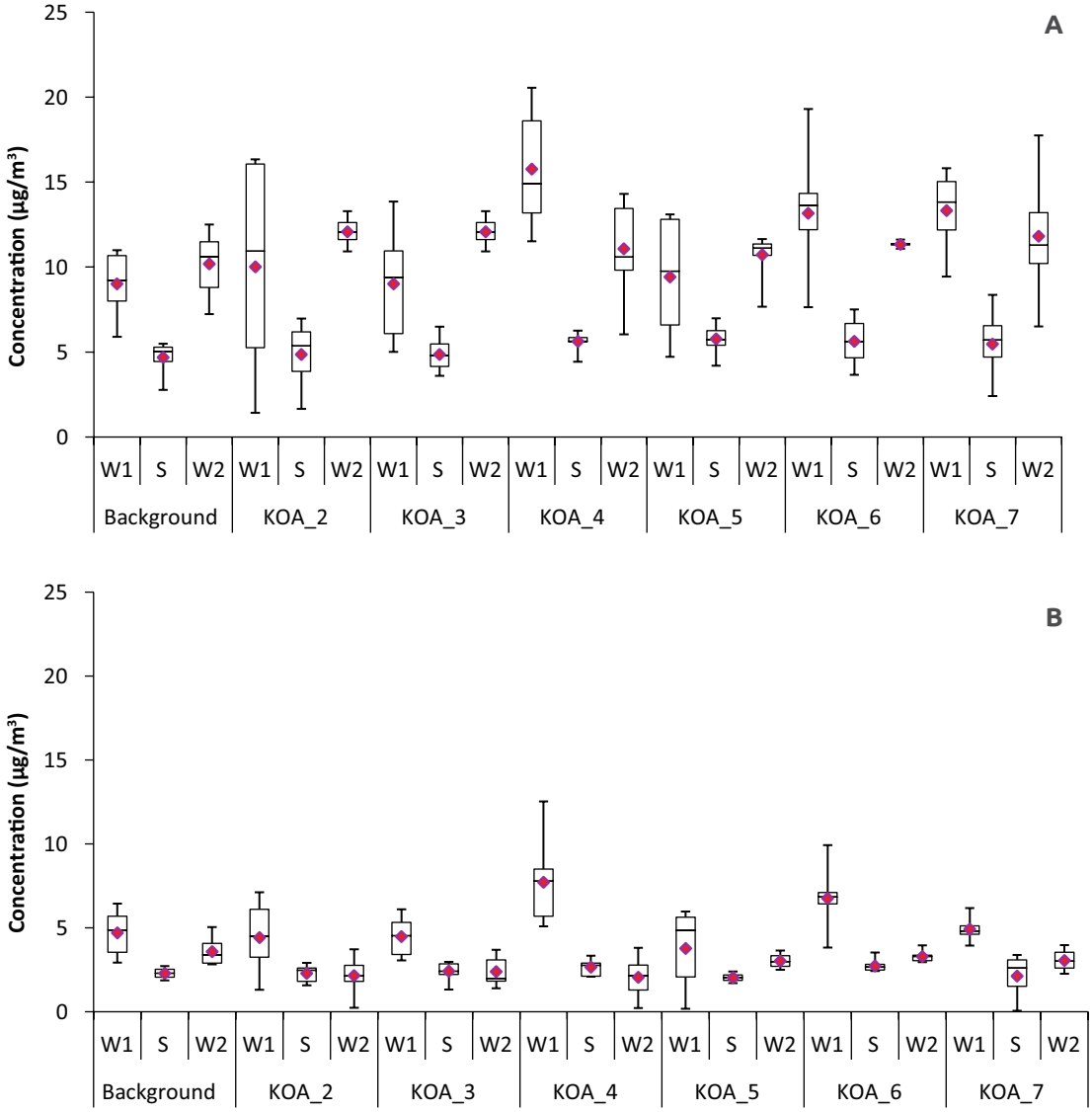

FIGURE 8 Atmospheric concentrations of BC (A.) and BrC (B.) at different AQM locations in the KMC area

The box shows the median of the dataset, with the first quartile representing 25% of the data below Q1, and the third quartile representing 75% of the data above Q3. The top whisker represents the maximum value, and the bottom whisker represents the minimum value.

***AQM locations - KOA_2**: Commercial 1; **KOA_3**: Commercial; **KOA_4**: Industrial; **KOA_5**: Residential; **KOA_6**: Residential; **KOA_7**: Kerb side. **W1**: Winter season (2022-23); **S**: Summer season (2023) and **W2**: Winter season (2023-24)*

residential cooking and industrial usage of biomass might have attributed to higher atmospheric BC concentrations at HWH_3.

The atmospheric BrC concentration varied between 1 µg/m³ and 7 µg/m³ at different AQM locations in the HMC area during the measurement period (Figure 9). The highest atmospheric

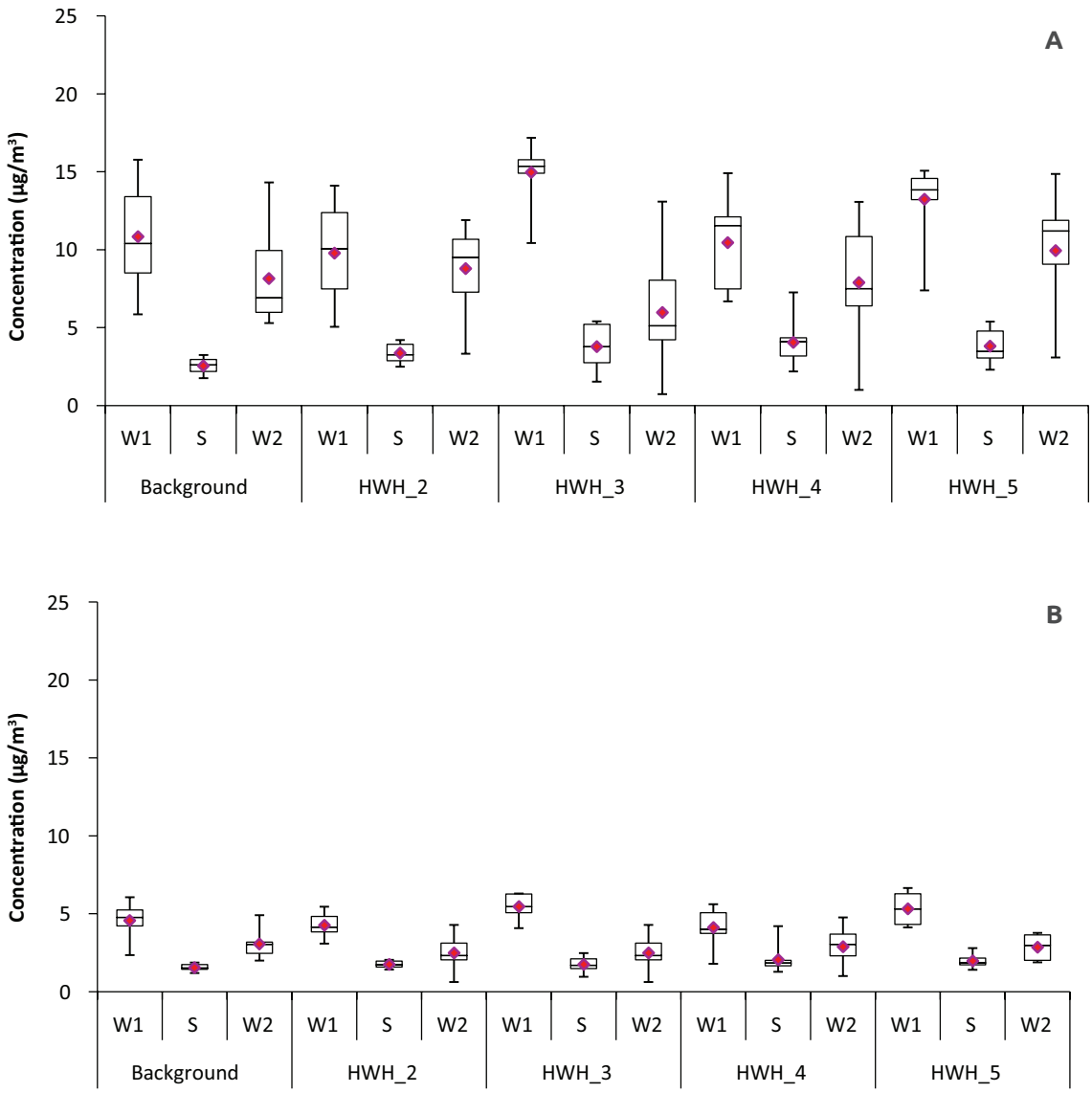

FIGURE 9 Atmospheric concentrations of BC (A.) and BrC (B.) at different AQM locations in the HMC area

The box shows the median of the dataset, with the first quartile representing 25% of the data below Q1, and the third quartile representing 75% of the data above Q3. The top whisker represents the maximum value, and the bottom whisker represents the minimum value.

AQM locations - HWH_2: Industrial; HWH_3: Residential; HWH_4: Kerbside; HWH_5: Commercial. W1: Winter season (2022-23); S: Summer season (2023) and W2: Winter season (2023-24)

concentration of BrC was recorded at HWH_5 during the W1 period. Local burning of refuse materials along with usage of biomass and coal in roadside eateries might have attributed to the highest atmospheric BrC concentration in the area. During the summer season, the BrC concentration varied between 1 µg/m³ and 5 µg/m³ while it varied between 2 µg/m³ and 7 µg/m³ during the W1 and between 1 µg/m³ and 6 µg/m³ during the W2 period (Figure 9).

TABLE 2 Spatiotemporal variations in atmospheric BC concentrations in the KMC area

	BC concentration (µg/m³)		
AQM location	**W1**	**S**	**W2**
Background	$9_a^B \pm 2$	$5_a^A \pm 1$	$10_a^B \pm 2$
KOA_2	$10_a^B \pm 6$	$5_a^A \pm 2$	$12_a^B \pm 1$
KOA_3	$9_a^B \pm 3$	$5_a^A \pm 1$	$12_a^B \pm 1$
KOA_4	$16_b^C \pm 3$	$6_a^A \pm 1$	$11_a^B \pm 3$
KOA_5	$9_a^B \pm 4$	$6_a^A \pm 1$	$11_a^C \pm 1$
KOA_6	$13_b^C \pm 4$	$6_a^A \pm 1$	$11_a^B \pm 1$
KOA_7	$13_b^B \pm 2$	$5_a^A \pm 2$	$12_a^B \pm 4$
Mean	$11^B \pm 4$	$6^A \pm 4$	$12^B \pm 8$

Mean±SD

In a column mean followed by a common alphabet (in subscript) is not significantly different at p<0.05 following Fisher's least significant difference (LSD) test. In a row mean followed by a common ALPHABET (in superscript) is not significantly different at p<0.05 following Fisher's least significant difference (LSD) test

AQM locations - KOA_2: Commercial 1; KOA_3: Commercial; KOA_4: Industrial; KOA_5: Residential; KOA_6: Residential; KOA_7: Kerb side. W1: Winter season (2022-23); S: Summer season (2023) and W2: Winter season (2023-24)

The mean atmospheric concentration of BC was significantly higher ($p < 0.05$) at HWH_3 (15 µg/m³) during the W1 period compared to other AQM locations in the HMC area (Table 3). However, there were no significant variations ($p > 0.05$) in atmospheric BC concentrations during summer and W2 period in the HMC area. The mean atmospheric BC concentration during summer season (4 µg/m³) was significantly lower than the winter season in the HMC area. There was a significant difference ($p < 0.05$) between the mean atmospheric BC concentrations during W1 and W2 period (Table 3).

TABLE 3 Spatiotemporal variations in atmospheric BC concentrations in the HMC area

	BC concentration (µg/m³)		
AQM location	**W1**	**S**	**W2**
Background	$11_a^B \pm 3$	$3_a^A \pm 1$	$8_a^B \pm 3$
HWH_2	$10_a^B \pm 4$	$3_a^A \pm 1$	$9_a^B \pm 3$
HWH_3	$15_b^B \pm 2$	$4_a^A \pm 1$	$6_a^A \pm 4$
HWH_4	$10_a^B \pm 3$	$4_a^A \pm 2$	$8_a^B \pm 4$
HWH_5	$13_a^B \pm 2$	$4_a^A \pm 1$	$10_a^B \pm 4$
Mean	$12^C \pm 3$	$4^A \pm 1$	$8^B \pm 4$

Mean±SD

In a column mean followed by a common alphabet (in subscript) is not significantly different at p<0.05 following Fisher's least significant difference (LSD) test. In a row mean followed by a common ALPHABET (in superscript) is not significantly different at p<0.05 following Fisher's least significant difference (LSD) test.

AQM locations - HWH_2: Industrial; HWH_3: Residential; HWH_4: Kerbside; HWH_5: Commercial. W1: Winter season (2022-23); S: Summer season (2023) and W2: Winter season (2023-24)

Sectoral Emission of Atmospheric Black Carbon

Sectoral emission of atmospheric BC is a database that details the amount of BC released into the atmosphere by a source over a given period. It contains all possible sources of the BC. This helps in understanding the spatiotemporal distributions of emissions from various sources within a region and critical inputs for building a regional action plan to manage the atmospheric concentration of BC.

The type of combustion greatly affects the BC emission rates; notably, inefficient combustion emits more BC than efficient combustion for the same type of fuel. Emission inventories of BC have been limitedly studied in India. Majorly studies on source-specific emission inventory of BC have been conducted at the national level. Simulated BC concentrations in India are 2 to 6 times lower than the observed concentrations (Ganguly *et al.*, 2009). Schultz *et al.*, 2007 estimated BC emissions in 2010 as 697 Gg whereas Klimont *et al.* (2009) reported BC emissions as 1104 Gg for the year 2010, and Lu *et al.* (2011) reported them as 1015 Gg for the year 2010. Again, for the year 2011, the System of Air Quality Weather Forecasting and Research (SAFAR) emission inventory (Sahu *et al.*, 2008) estimated BC emissions as 1119 Gg, and Paliwal *et al.*, (2016) estimated BC emissions as 901.11 ± 151.56 Gg. IGP is the main contributor to national BC emissions. The high dependence on biomass fuels and the presence of the brick and sugar industry accentuates the emissions from this region. National BC emission was estimated as be 901 ± 152 Gg yr^{-1} (Paliwal *et al.*, 2016). They also reported that with annual emissions of 140 Gg, the state of Uttar Pradesh emits the most in the IGP followed, by West Bengal (57.67 Gg), Bihar (47.8 Gg), Punjab (34.01 Gg), Haryana (26.82 Gg), and the National Capital Territory (NCT) of Delhi (6.74 Gg). The residential sector (628 Gg) contributes the most, followed by industry (261 Gg), and transport (136 Gg) (Klimont *et al.*, 2009). Additionally, Lu *et al.*, (2011) reported that residential fuel burning (579 Gg) contributes the highest BC emissions, followed by industry (227 Gg), transport (111 Gg), and crop residue burning (74 Gg) in India. Firewood was reported as the single-largest emitter, with 177 Gg (20%) of BC emissions in 2011 (Paliwal *et al.*, 2016).

The basic equation followed in the study to estimate the BC emissions from different sectors is,

$$E_P = \sum_s \sum_f A_{s,f} \times EF_{p,s,f} \qquad \text{eq.3}$$

where Ep is the annual emission of a pollutant (p); s is the sector; f is the type of fuel; A is the activity data (fuel consumption or other emission-related data); EF is the emission factor of the pollutant (p).

As mentioned in the Background section of this report, the sectoral activity data ($A_{s,f}$) estimated from the survey conducted during the air pollution source apportionment and atmospheric carrying capacity study in Kolkata and Howrah was used in the estimation of sectoral BC emission.

The KMC and HMC areas were distributed into a 2 km × 2 km domain(Figure 10) based on the grids used in the air pollution source apportionment and atmospheric carrying capacity study in Kolkata and Howrah, to keep a consistency between the two studies and ease of incorporation of the sectoral activity data (As,f) from the earlier study.

Sector-specific Annual Emissions of Atmospheric Black Carbon

The major sources of atmospheric BC were grouped into two broad categories: i) The energy use sectors and ii) No energy use sectors, to prepare the emission inventory of the study domain vis-à-vis the KMC and HMC areas. The sectors that consume large quantities of fuels in any form are listed in the 'energy-use sector' – a) Residential, b) Industry, c) Power, d) Transport, and e) Restaurants/Eateries. The air pollution emissions sources that do not consume fuel but still contribute to air pollution emissions are listed in the 'no energy use sector' – a) Refuse material burning, b) Landfill fire, and c) Cremation activities.

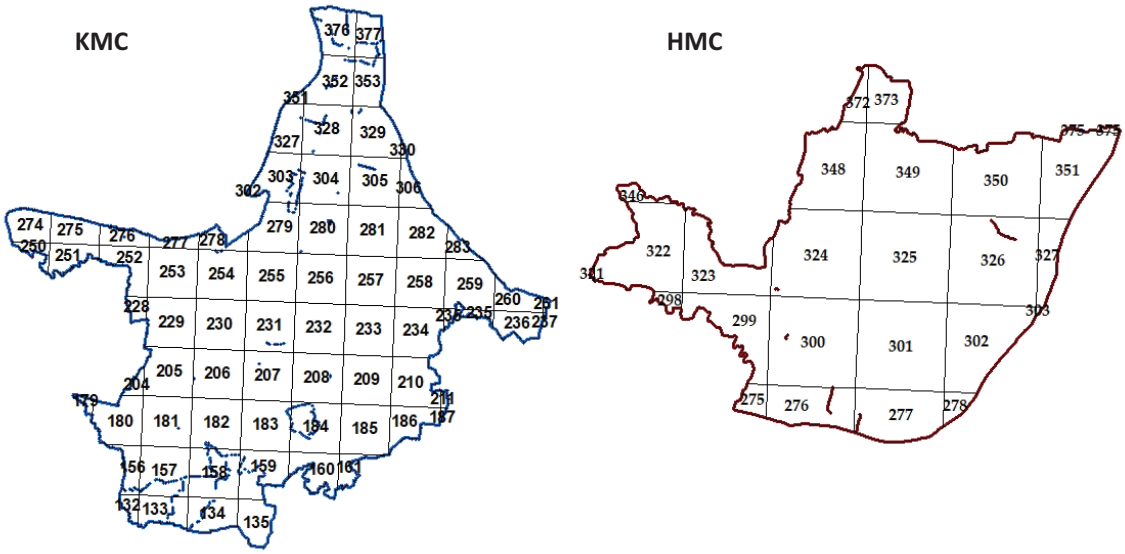

FIGURE 10 2 km × 2 km grids of the KMC and HMC areas

Residential sector

BC emission from the residential sector is dependent on the fuel consumed in residential households for cooking, heating, and lighting activities. Since the average wintertime temperature does not drop below 15°C in the study domain, space heating is not a common practice in the area. Additionally, the households in the area are mostly connected to power grid and power cut is also very occasional in the area, so there is very minimal use of fuel for lighting purposes in the

residential households. The fuel specific emission factors ($EF_{p,f,s}$) of BC for the residential sector (Table 4) were used in eq. 1 to prepare the sectoral emission inventory.

TABLE 4 Emission factors (g/kg) of BC from different fuel types used in the residential sector

	Firewood	Dung cake	Crop residue	Coal	Kerosene	LPG
g/kg	0.4*	-	-	0.08**	0.6***	-

**Saud et al. (2012); **Huy et al. (2021); ***Lu et al. (2011)*

Annual black carbon emission from the residential sector in the Kolkata Municipal Corporation area

The estimated annual consumption of different types of fuels in slum households of the KMC area during 2023 followed the order: Firewood (147271 t) > Kerosene (36061 t) > LPG (24888 t) > Coal (12526 t) (TERI, 2025a). About 60 t/annum BC emission was estimated from the burning of firewood in the residential sector followed using kerosene for cooking (Figure 11).

The spatial distribution of BC emissions from the residential sector suggests no emissions from some grids in the southern part of the city. This is attributed to 100% LPG uses for residential cooking in these areas. The highest BC emissions were estimated towards the northern side of the city particularly in the slum areas of the east and west canal areas, Cossipore area and Kumartuli area (Figure 12).

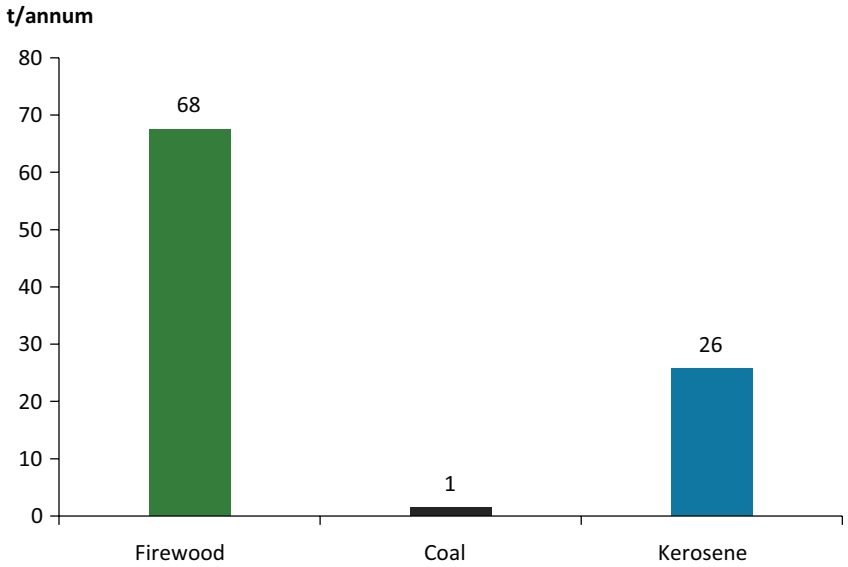

FIGURE 11 Fuel-wise emission of BC from the residential sectors in the KMC area

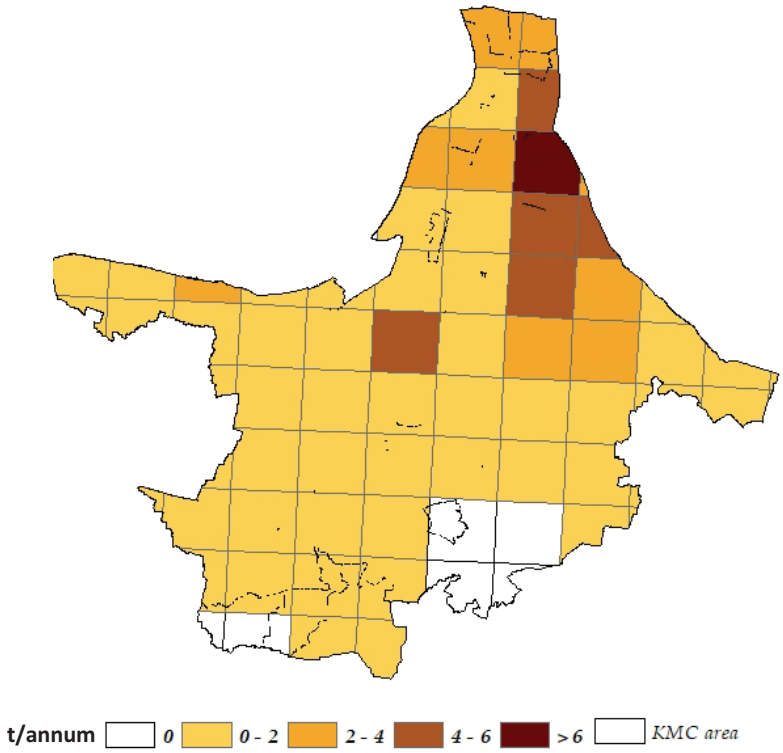

FIGURE 12 Spatial variation of BC emissions from the residential sectors in the KMC area

Annual black carbon emission from the residential sector in the Howrah Municipal Corporation area

There are about 733 slums in the HMC area spread over municipal land, railway land, and private lands. About 8% of the total population of the HMC area lives in slums (District Census Handbook of Howrah, 2014). Estimated annual consumption of different types of fuels at the slum households in the HMC area followed the order: Fuelwood (11138 t) > Coal (2622 t) > LPG (2277 t) > Kerosene (2266 t). On the other side, the annual consumption of different types of fuels for cooking activity at the non-slum households in the HMC area followed the order: Coal (49403 t) > LPG (39959 t) > Firewood (18807 t) > Kerosene (12056 t) (TERI, 2025b). Annual BC emissions from the residential sector in the HMC area were estimated as 25 t/annum which is much lower than that of the KMC area. However, the estimated BC emission from coal use in the residential sector in the HMC area was much higher than that of the KMC area (Figure 13). Spatial distribution of the estimated BC emission from the residential sector suggests comparatively higher emissions from the Salkia, Bandha Ghat, and Howrah Maidan areas (Figure 14), this may be attributed to the presence of many slum areas in the region and the use of coal and firewood in the slums for residential cooking.

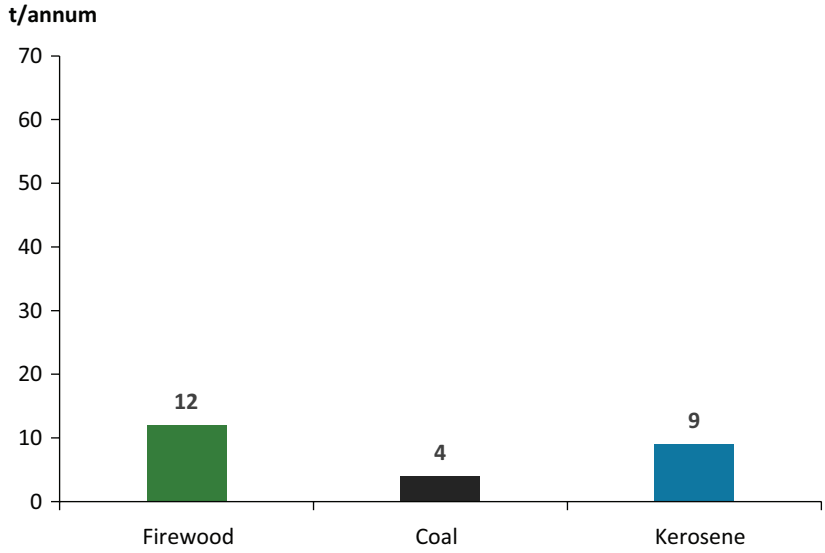

FIGURE 13 Fuel-wise emission of BC from the residential sectors in the HMC area

Transport sector

Vehicular tailpipe emissions are a significant contributor to air pollution in Indian cities, with BC being one of the most harmful pollutants released by the transport sector. BC is primarily emitted from diesel-powered vehicles, such as trucks and buses.

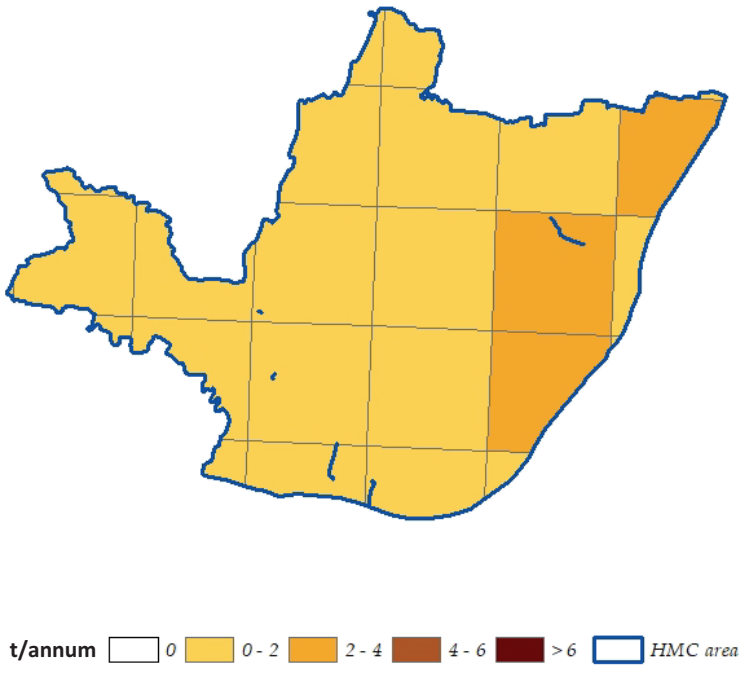

FIGURE 14 Spatial variation of BC emissions from the residential sectors in the HMC area

BC emissions from the transport sector in Kolkata and Howrah were estimated using the fuel used per kilometre travelled approach, involving an artificial intelligence (AI)-driven vehicular survey on different roads of Kolkata and Howrah cities (TERI, 2025a). Norm-wise distribution of vehicular categories, number of vehicles on different types of road, length of different types of roads and fuel type of vehicles were used to estimate the fuel consumption in each city.

Fuel-wise BC EF of different types of vehicles for this exercise are adopted from the GAINS Asia (Table 5).

TABLE 5 Vehicle category and fuel type-wise emission factors of BC

Category	Fuel type	Emission factor (t/PJ)
Bus	CNG	1
	LPG	0
	Diesel	53
Truck	CNG	1
	LPG	0
	Diesel	53
3W	CNG	0
	Petrol	75
Car	CNG	0
	Petrol	1
	LPG	0
	Diesel	73
LCV	CNG	0
	Petrol	1
	Diesel	58
2W	Petrol	2

Source: GAINS-Asia

Annual black carbon emission from the transport sector in the Kolkata Municipal Corporation area

The estimated vehicular profile indicates cars and jeeps are primarily in the BSIV category, accounting for 69%, while buses are also more prevalent in BSIII with 50% (Figure 15). The presence of BSVI norm vehicles is relatively lower across all categories of vehicles, indicating that newer vehicles are still gaining traction in the KMC area.

The road network in the KMC area was mapped using ArcGIS 10.8.2. The roads were categorized into; i) Major, ii) Connecting, and iii) Local based on the width and nature of the road (Figure 16).

In Kolkata, total BC emissions amount to 2754 t/Annum, with buses alone accounting for nearly 69% of these emissions. This high contribution is due to the continuous operation of buses,

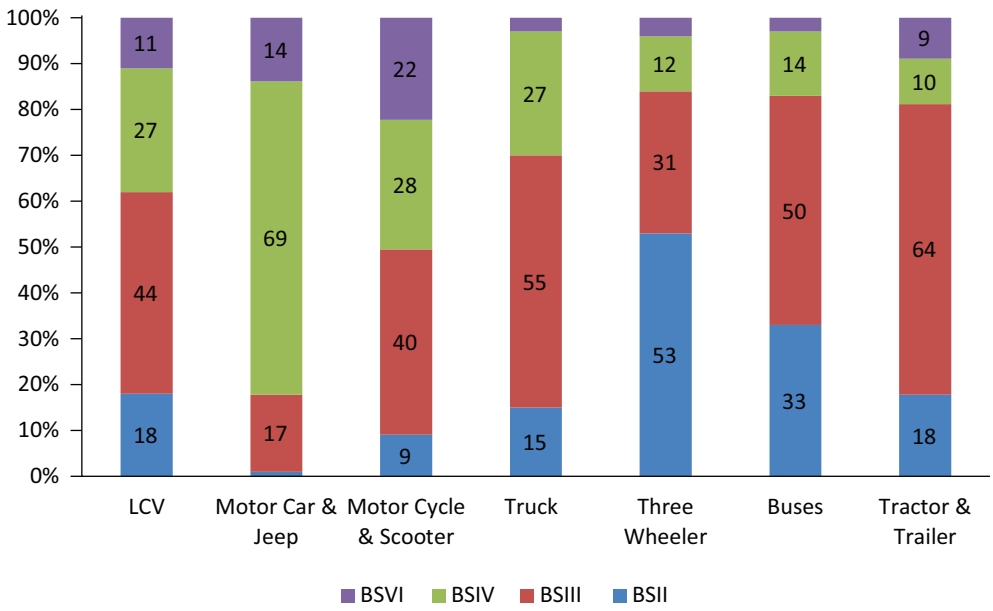

FIGURE 15 Estimated BS-norm-wise distribution of different vehicle categories in the KMC area

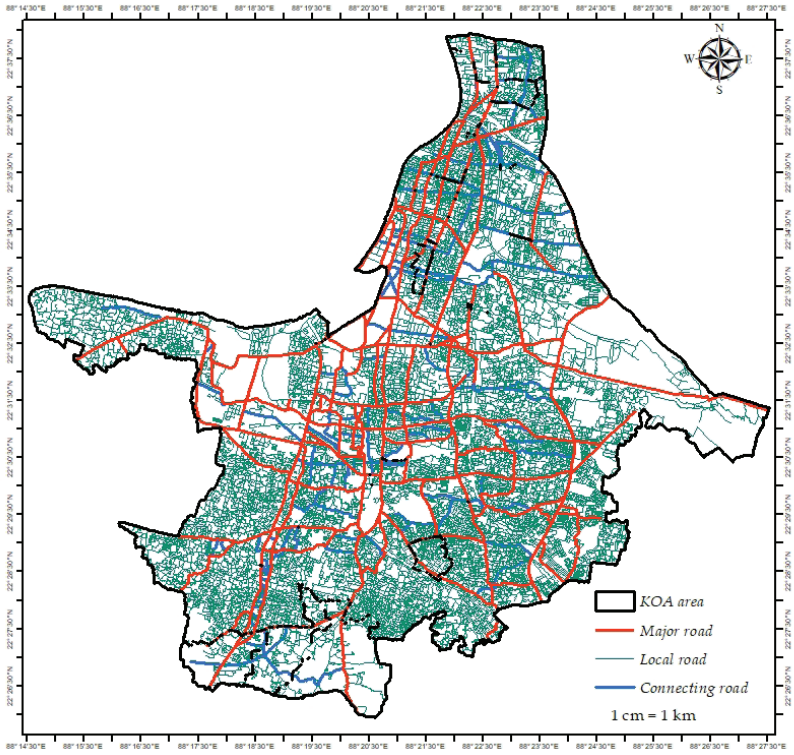

FIGURE 16 Road network in the KMC area

especially diesel-fueled ones, which are a major part of public transport in the city. Two-wheelers (2W) also contribute significantly, adding 544 t/Annum (20%) to total BC emissions, as they are one of the most common vehicle types. Trucks are another major source, contributing 156 t/annum (5.6%), due to freight movement within the city. Meanwhile, car and light commercial vehicles (LCVs) contribute relatively smaller amounts, with emissions of 2 t/annum and 5 t/annum, respectively. While 2W and 3W contributes 544 t/annum and 151 t/annum, respectively.

TABLE 6 Estimated emissions of BC from different categories of vehicles in the transport sector of the KMC area

	Truck	Bus	Car	2W	3W	LCVs	Total
t/annum	156	1896	2	544	151	5	2754

Annual black carbon emission from the transport sector in the Howrah Municipal Corporation area

The estimated vehicular profile indicates cars and jeeps are primarily in the BSIV category, accounting for 72%, while buses are also more prevalent in BSIII with 53% (Figure 17). The presence of BSVI norm vehicles is relatively lower across all categories of vehicles, indicating that newer vehicles are still gaining traction in the HMC area.

The road network in the HMC area was mapped using the ArcGIS 10.8.2. The roads were categorized into; i) Major, ii) Connecting, and iii) Local based on the width and nature of the road. Total lengths of the major, connecting and local road in the HMC area were estimated as 175 km, 77 km, and 1158 km, respectively (Figure 18).

Total estimated BC emissions from the transport sector in the HMC area was 1330 t/annum, with buses as the dominant source, contributing 910 t/annum (68%). The second-largest source is

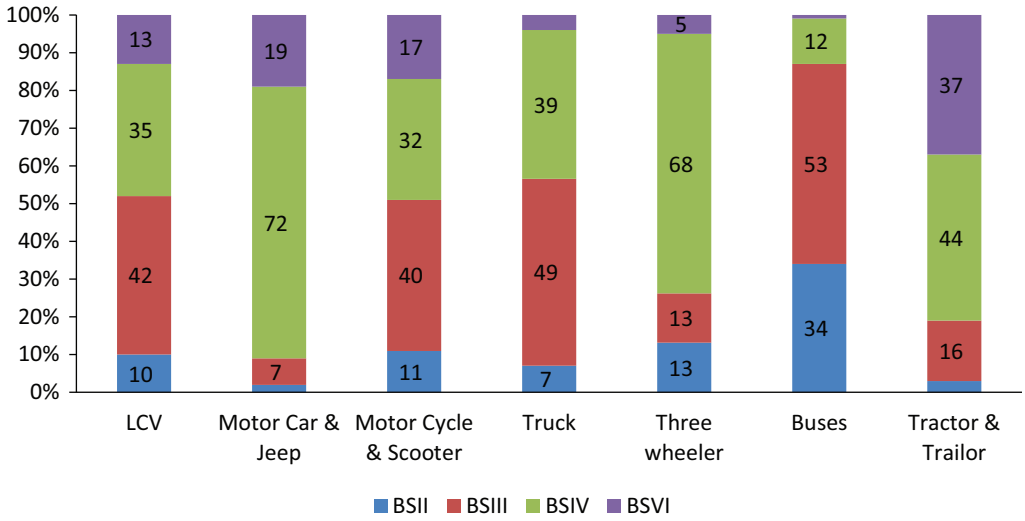

FIGURE 17 Estimated BS-norm-wise distribution of different vehicle categories in the HMC area

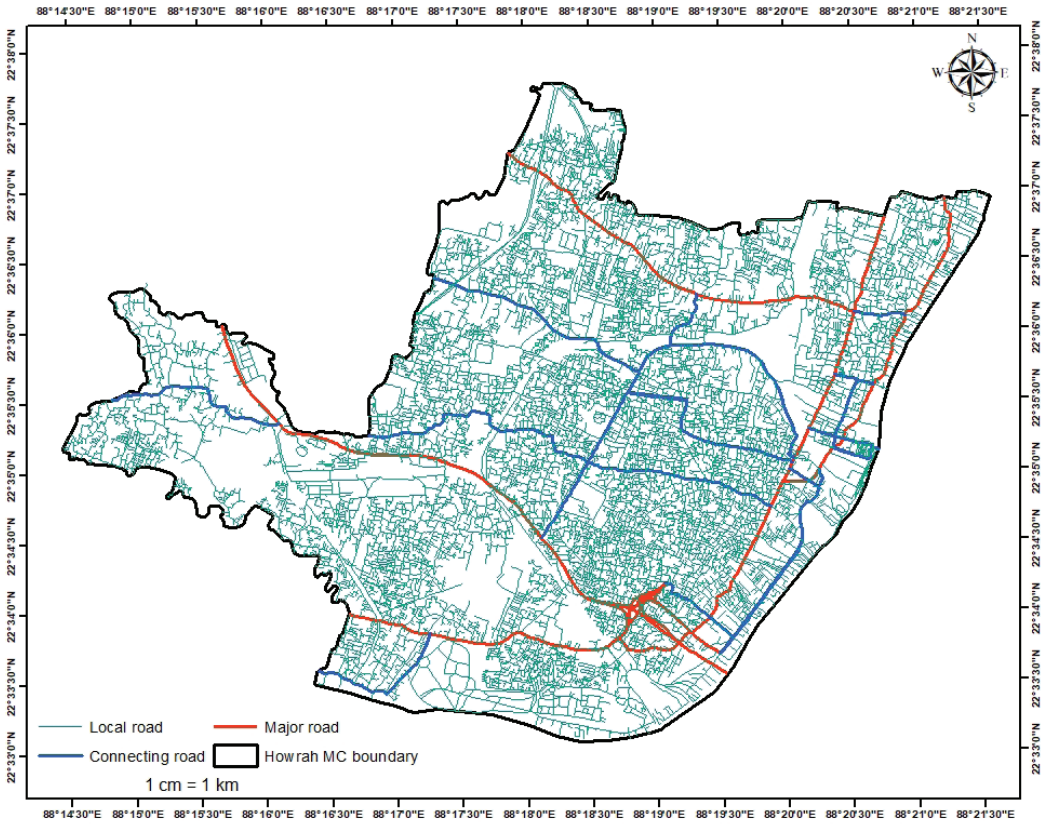

FIGURE 18 Road network in the HMC area

two-wheelers (2W), which contribute 191 t/annum (14%), followed by trucks 220 t/annum (16%). The estimated emissions of BC from three-wheelers (3W) and LCVs are minimal, accounting for 3.4 t/annum and 4.8 t/Annum, respectively. Cars have the lowest BC emissions in Howrah, at just 0.36 t/annum.

TABLE 7 Estimated emissions of BC from different categories of vehicles in the transport sector of the HMC area

	Truck	Bus	Car	2W	3W	LCVs	Total
t/annum	220	910	0.4	191	3.4	4.8	1330

Nearly 2.5 times higher annual BC emissions were estimated from the transport sector in Kolkata than that of Howrah, likely due to a larger vehicle fleet, more traffic congestion, and higher fuel consumption. The higher contribution of buses in both cities suggests that interventions such as transitioning to cleaner fuels, and electrification of public transport could significantly reduce BC emissions.

Spatial variations in black carbon emission from the transport sector in the KMC and the Howrah Municipal Corporation areas

The length of each type of road in the 2 km × 2 km grids (Figure 10) of the Kolkata Municipal Corporation and the HMC areas were estimated from the mapped road network in the KMC (Figure 16) and the HMC areas (Figure 18).

The spatial distribution of BC emissions from the transport sector suggests that the gridded emissions are higher in the central region of the KMC area compared to other areas (Figure 19). This is attributed to higher traffic volume in the region, mainly the 2W and buses.

The estimated BC emissions were higher in the central area of the HMC, covering the Howrah station, Howrah maidan, hospital, and court areas. The major emissions of BC were estimated from the 2W, 3W, and buses in these areas.

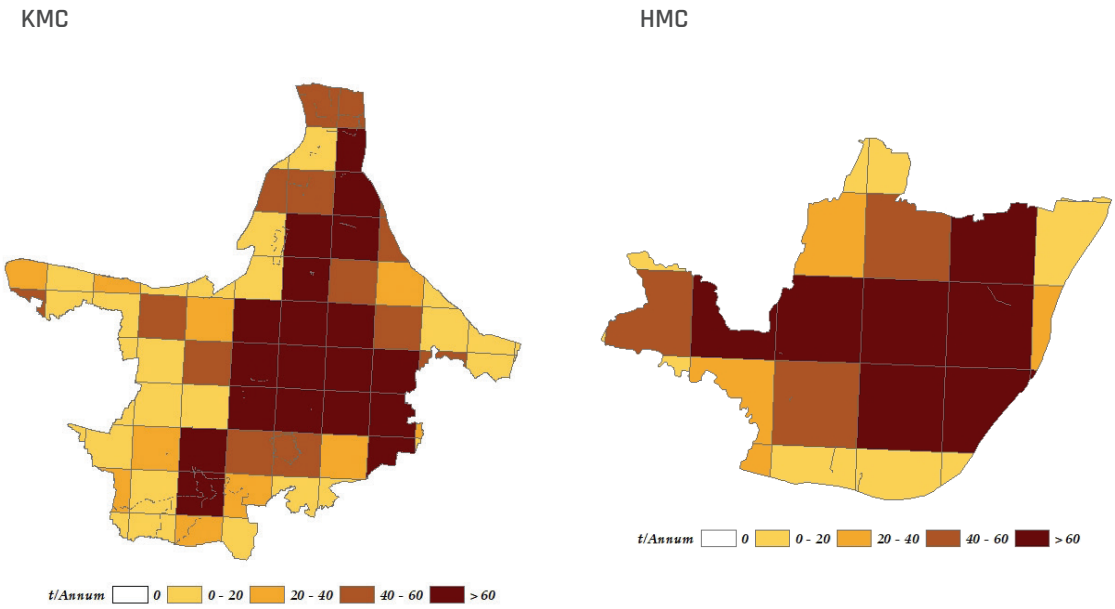

FIGURE 19 Spatial distribution of BC emission from the transport sector in the KMC and the HMC areas

Industry sector

Both cities have long been regarded as important industrial centres in India. The domain, which is located on the banks of the Hooghly River, has a long history of industrial development that began during the colonial era when Calcutta was the capital of British India until 1911. By making use of its advantageous location along the Bay of Bengal and with access to inland waterways, the city became a hub for trade and industry throughout this period. Kolkata has changed throughout time from being a hub for traditional industries to a contemporary city that faces difficulties with urbanization and industrial diversification. In the present study, the red and orange category

industries were considered to estimate emissions from the industrial sectors in the KMC and the HMC areas. Industry-wise fuel use data of different industries in the KMC and the HMC areas were collected from TERI (2025a,b). Fuel-specific emission factors were used following GAINS-Asia (Table 8).

TABLE 8 Fuel-wise emission factors of BC emission from the industry sector

	Coke	Briquettes	Natural gas	Coal	Kerosene	LPG	Diesel	Firewood	Other biomass*
t/PJ	0.52	0.52	0.01	7.89	0.74	0.01	0.11	9.6	14.2

*Other biomass includes processed agroresidues like rice husk, nut shell, etc.

Annual black carbon emission from the industry sector in the Kolkata Municipal Corporation area

The industries in the city are mostly located in the northern corner and the western side of the city – towards Khidirpur and Gardenrich areas. It was estimated that about 7150 tonnes of coal, 44 ML of liquid fuel and 26463 m^3 gaseous fuels are consumed in the industries in the KMC area, annually (TERI, 2025a). Annual BC emissions from the industries in the KMC area were estimated as 0.00004 Kt of which about 83% was estimated from the combustion of solid fuel.

Annual black carbon emission from the industry sector in the Howrah Municipal Corporation area

Manufacturing, metal-processing, paint, and engineering-related industries are the key industry types in the HMC area. There are large numbers of micro, small, and medium enterprises in the HMC area. There are 357 red or orange category industries in the HMC area. These industries are mostly located around Benaras Road (Figure 20) in the northern side of the HMC area. Paint and jute industries are mostly located on the bank of the Hooghly River.

It was estimated that about 2.6 Mt of solid fuels are used in the industry sector in the HMC area annually. About 1.5 Mt of coke is consumed annually in the industries in the HMC area. In addition, about 101 Kt of coal and 68 Kt of biomass are also consumed in the industries in the HMC area annually. Among the liquid fuels, about 19 ML of HSD and 17 ML of LSD are consumed in industries annually, while about 3.7 Mm^3 gaseous fuels are consumed annually in the industries in the HMC area (TERI, 2025b).

About 0.05 t of BC emission from industries was estimated annually in the HMC area, of which more than 45% was estimated from the solid fuel use in the industries, followed by about 36% of the use of liquid fuel in industries in the HMC area.

Spatial variations in black carbon emission from the industry sector in the Kolkata Municipal Corporation and the Howrah Municipal Corporation areas

In the KMC area, the estimated emissions of BC from the industries were mostly below 0.00004 t/annum, except in the Khidirpur area where the concentration was above 0.00008 t/annum

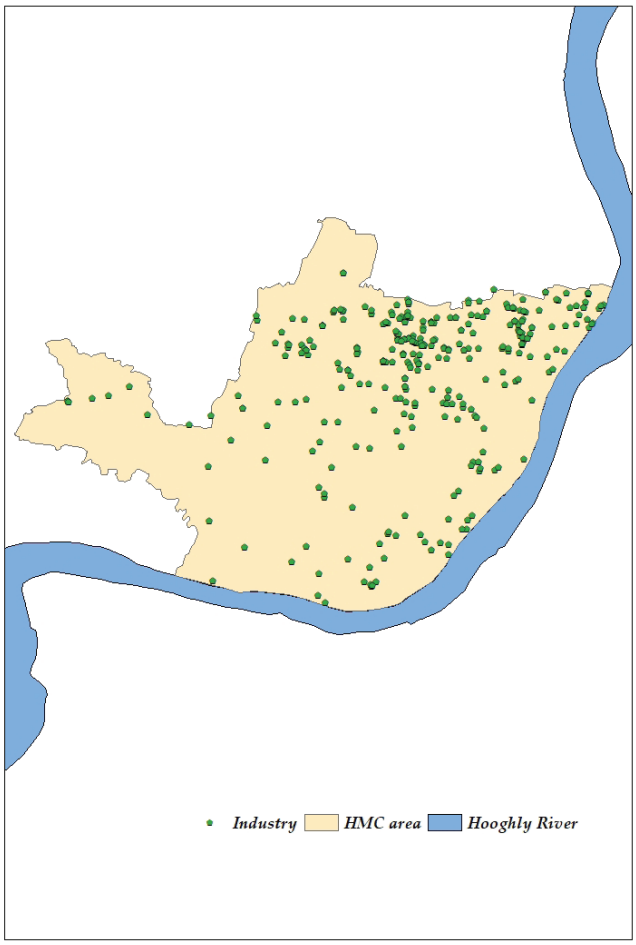

FIGURE 20 Spatial distribution of red and orange categories industries in the HMC area

(Figure 21). The higher emissions of BC in the western side of the city are mainly attributed to large-scale coal use in industries.

Spatial distribution of estimated annual particulate and gaseous pollution emissions from the combustion of fuels in industries in the HMC area suggest that the major emissions were from the Benaras Road and Salkia area towards the northern side of the city (Figure 21).

Power sector

The diesel generator (DG) sets are generally used as a backup to the power supply during load shedding. However, long power cut is not a general phenomenon in the KMC and HMC areas. However, uninterrupted or essential operations in sectors like hospitals, industries, IT centres, and commercial establishments (e.g. banks, etc.) generally use diesel generator sets (DG sets) as the primary power supply or backup source of power supply. Emissions from the DG set operation

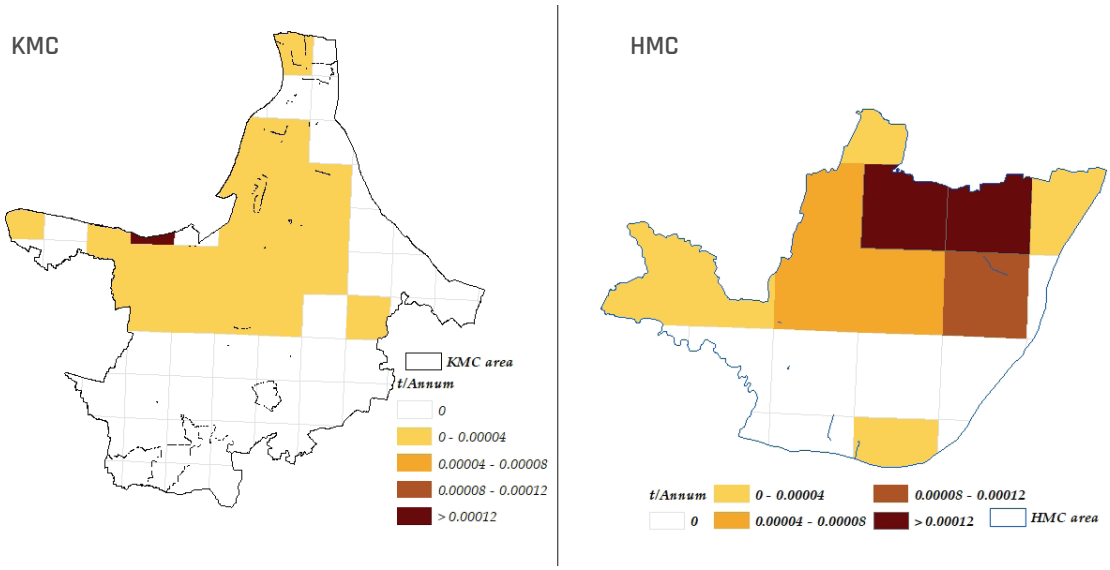

FIGURE 21 Spatial distribution of BC emission from industries in the KMC and HMC areas

depend on the capacity of the DG set, quality and amount of fuel consumption, and operational hours of the DG set.

75% of the $PM_{2.5}$ (113.3 ng/J) (USEPA, 2022) emissions from the DG set was considered as BC (EPA, 2012). The $PM_{2.5}$ emission control efficiency of the DG set was applied to the ***eq. 3*** wherever, Air Pollution Control Devices (APCDs) are installed with the DG set.

Estimated black carbon emission from the diesel generator set operation in the Kolkata Municipal Corporation area

According to the data collected from the WBPCB, there are 104 industries that are using DG sets of different capacities. The capacity of the DG set in industries in the KMC area varied from 7.5 KVA to 1400 KVA. In addition, there are large DG set operations in 208 hotels, 101 hospitals, and 23 offices registered with the WBPCB.

Annual BC emission from the DG set operation in the KMC area was estimated as 51 t/annum following the capacity of individual DG set (TERI, 2025a) and the emission factors mentioned above.

Estimated black carbon emission from the diesel generator set operation in the Howrah Municipal Corporation area

The data collected from the WBPCB (Howrah RO) suggests 167 industries in the HMC area are using DG sets. The capacity of these DG sets varies between 20 KVA to 1250 KVA. In the HMC area, 21 and 54 hotels and hospitals, respectively use the DG sets registered with the WBPCB (capacity: 12 KVA to 1000 KVA). Ten offices have DG sets with capacity between 8 KVA to 15 KVA in the HMC area (TERI, 2025b).

Accordingly, the annual BC emission from the DG set operation in the HMC area was estimated as 25 t/annum following the capacity of the individual DG set and the emission factors mentioned above.

Eateries, restaurants, and bakery

The use of solid fuel for cooking in roadside eateries and restaurants is a common practice in areas where clean fuel alternatives are limited or unaffordable. In addition to the emission of air pollutants, the use of coal, wood, and kerosene in restaurants and roadside eateries releases a substantial amount of BC. Like the residential sector, the restaurant and eat-out sectors are a considerable contributor to BC emissions, especially in urban areas.

In the KMC and HMC areas, restaurants and eateries rely heavily on solid fuels for cooking. Firewood was identified as the primary fuel contributing to BC emissions in the KMC area, whereas coal was the dominant fuel used in the HMC area (TERI, 2025a,b).

The EFs used to estimate BC emissions from coal, firewood, and kerosene in the restaurant and eat-out sectors were derived from the same source as those applied in the residential sector. This assumption was based on the similarity in combustion processes and cooking practices observed in both sectors.

In 2023, the BC emissions from restaurants in the KMC area were estimated at 0.9 t/annum, while emission from the eateries was estimated at approximately 2.5 t/annum. On the other hand, restaurants in the HMC area were estimated to contribute 0.14 t of BC, and eateries accounted for 0.36 t of BC annually.

Refuse materials burning

Open burning of refuse materials is a common practice in areas lacking adequate waste management infrastructure. In addition to the emission of air pollutants, uncontrolled burning of waste in open fires releases a substantial amount of BC into the atmosphere. Refuse burning activity is prevalent in the KMC and the HMC areas. The quantity of refuse material burned depends on the quantity of waste that remains uncollected. The uncollected fraction of refuse material was estimated based on the quantity of waste generated and collected in the KMC and HMC areas, respectively. Accordingly, the amount of refuse material burned along with the emission factor of BC is used to estimate the emission of BC from the open burning of waste materials. The EF of BC from the burning of refuse material considered for the study is 0.65 g/kg (Woodall *et al.* 2012).

Annual emissions of BC from the burning of refuse materials in the KMC and HMC areas were estimated as 79 t and 30 t, respectively. The combustion process and the character of the associated BC emissions are strongly dependent upon the physical conditions of the combusting material. BC emissions from open waste occur primarily due to incomplete combustion of refuse substances, namely biomass (dry leaves), plastics, paper, textiles, rubber, etc. Generally, the

composition of refuse substances is complex in nature and can differ in moisture content, particle size distribution, and density. Materials such as biomass, plastics, and rubber contain high levels of carbon and can release significant amounts of BC during incomplete combustion.

Crematorium

In a large Indian metropolis, the crematoria constitute an unusual source of air pollution. Smoke and emissions from these unorthodox sources of air pollution exacerbate the air pollution challenge in a vibrant, cosmopolitan city. But despite their importance, these ancient locations for ceremonial fire are mostly disregarded as the city struggles with population development and industrialization. Although burning incense on pyres is a common ethnic ritual, it degrades the local air quality.

The primary cause of the air pollution from the crematorium is the conventional wood pyre-based cremation. There are gas and electric crematoria; however, the current inventory does not account for their emissions.

Based on the wood consumption in each pyre, annual wood consumption in the KMC and HMC areas was calculated (TERI, 2025a,b). The wood consumption and the EF (0.52 g/kg) (Akagi *et al.*, 2011) were used to estimate the annual BC emission from the cremation activities in the KMC and the HMC areas. It was estimated that about 0.5 t/Annum and 2t/Annum of BC were emitted from the pyre cremation activities in the KMC and the HMC areas, respectively.

Spatial variation of estimated annual black carbon emission

Annual BC emissions from the KMC and the HMC areas were estimated to be 3103 t/annum and 1417 t/annum, respectively. The transport sector was estimated as the major source of BC emission in the KMC (2754 t/annum) and the HMC (1248 t/annum) areas.The estimated spatial variation of BC emissions in the KMC area ranged between 0.001 t/annum and 134 t/annum (Figure 22). Higher emissions of BC were estimated in the central and northern regions of the KMC area, mainly due to the emissons from the residential and the transport sectors. Emissions of BC were attributed to the landfill fire towards the eastern side of the city–the Dhapa landfill area located at grid number 259 (Figure 10) (Table 9).

Landfill fire was estimated as the second-largest source of BC in both cities. Industrial emissions were estimated as the smallest source of BC in both KMC and HMC areas.

The estimated spatial variation of BC emissions in the KMC area ranged between 0.01 t/annum and 134 t/annum (Figure 22). Higher emissions of BC were estimated the central and northern regions of the KMC area, mainly due to the emissions from the residential and the transport sectors. Emissions of BC was attributed to the landfill fire towards the eastern side of the city–the Dhapa landfill area located at grid number 259 (Figure 10).

TABLE 9 Sector-wise estimated annual emission of BC (t/annum) in the KMC and HMC areas

Sector	t/annum	
	KMC area	HMC area
Residential	95	25
Industrial	0.0004	0.0046
Transport	2754	1330
Power (diesel generator)	51	25
Restaurant, eateries, bakery	3	1
Refuse material burning	79	30
Landfill fire	119	35
Crematoria	1	2
Total	3103	1417

The estimated annual BC emissions were ranged between 0.8 t/annum and 177 t/annum at different grids in the HMC area. Higher emissions were estimated in the grid covering Howrah station, Howrah Maidan, Belgachia in the central and northern regions of the city (Figure 22).

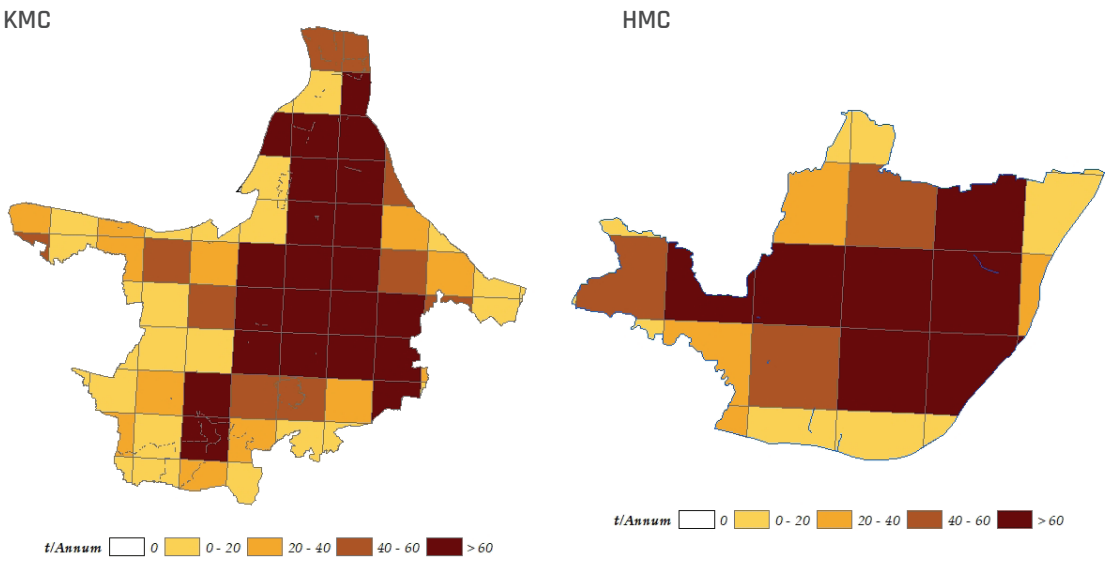

FIGURE 22 Spatial distribution of annual BC emissions in the KMC and the HMC areas

Simulated Spatial Variation of Atmospheric Black Carbon Concentration

Understanding the impact of BC in urban environments requires a thorough assessment of its concentration, as well as its spatial and temporal variations. This can be achieved through measurements taken from both stationary and mobile platforms; however, obtaining a comprehensive perspective is challenging due to limitations in site coverage, time, and financial resources. Although low-cost BC sensors facilitate air quality monitoring for localized studies (Savadkoohi *et al.*, 2023), integrating model development with observational datasets remains crucial for in-depth analysis and accurate forecasting.

Land-use regression, a method that relies on linear regression models, has been effectively used to estimate BC concentrations at the road level. For instance, in Ghent, Belgium, mobile monitors equipped with GPS devices have been employed to predict BC concentrations (Van den Hove *et al.*, 2019). Similarly, a machine learning-based non-linear approach has been introduced in Barcelona, Spain, to address data gaps in air quality records, allowing for reliable BC concentration estimations (Wai *et al.*, 2022).

Another widely used technique is the RLINE model, which employs a Gaussian dispersion formulation to simulate pollutants such as NO_x and BC from roadway emissions, as demonstrated in studies conducted in the San Francisco Bay Area (Patterson and Harley, 2019). On a broader scale, chemical transport models like Community Multiscale Air Quality Model (CMAQ) (Huang *et al.*, 2023) and Weather Research and Forecasting (WRF)-Chem (Rahimi *et al.*, 2020) are valuable tools for analyzing the spatial and temporal dynamics of BC. However, compared to the previously mentioned models, they require significantly greater computational resources and processing time. Building on these approaches, the WRF-CMAQ modelling framework has been utilized to estimate atmospheric BC concentrations by integrating meteorological and chemical transport simulations (Figure 23).

The CMAQ, part of the Models-3/CMAQ suite, unlike other atmospheric models employs a eulerian framework. It is designed to simulate the chemical transport of various pollutants under prevailing meteorological conditions (Byun and Ching, 1999). The CMAQ is widely regarded as a leading air quality model, particularly for assessing ozone (O_3) and aerosols (Byun and Schere, 2006). One of the key strengths of CMAQ is its ability to simulate the chemical behaviour of reactive species, such as ozone, nitrogen oxides (NO_x), hydrocarbons, and secondary particulates like sulfates and nitrates. Another major advantage of CMAQ is its multi-pollutant approach. Unlike

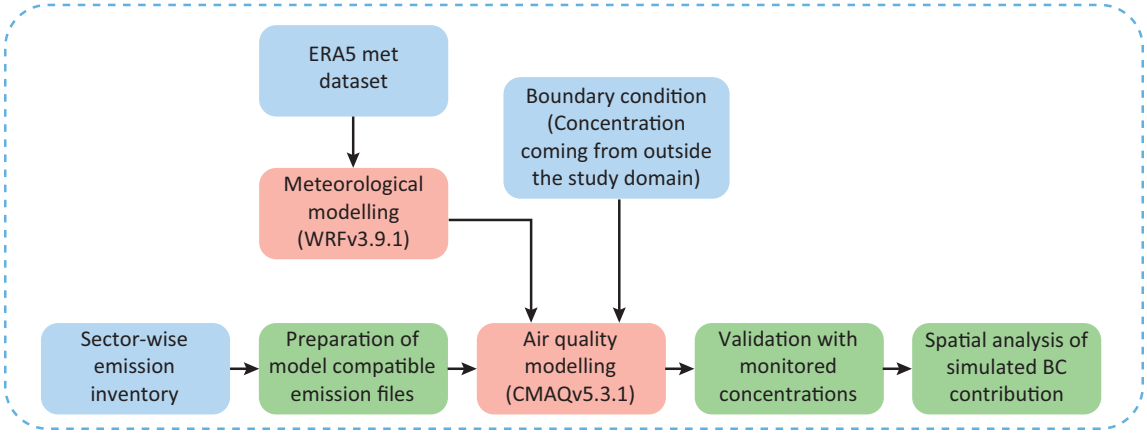

FIGURE 23 The WRF-CMAQ modelling framework to simulate atmospheric BC concentration

traditional models, which typically focus on individual pollutants, CMAQ considers interactions among multiple pollutants simultaneously. Furthermore, it accounts for complex photochemical reactions which are critical factors in the formation of secondary aerosols in the atmosphere.

This capabilities of CMAQ enables it to provide a more comprehensive understanding of the formation and transport of pollutants. Additionally, CMAQ can operate across a wide range of spatial scales, from continental to local, making it suitable for analyzing both long-range and medium-range pollutant transport. The WRF-CMAQ modelling setup is particularly advantageous for capturing the influence of meteorology on BC dispersion, assessing long-range transport, and identifying source contributions at a regional scale. Compared to statistical models and dispersion-based approaches, WRF-CMAQ offers a more process-based understanding of BC dynamics, making it a powerful tool for policy-relevant air quality assessments. Through this framework, ambient BC concentrations can be estimated with higher spatiotemporal resolution over large spatial domains, providing insights that support regulatory strategies and mitigation efforts.

The WRF-CMAQ modelling system is extensively employed in both policy-oriented and academic research, with applications across a range of geographical settings, including the Mediterranean Basin (Paza *et al.*, 2013), London (Sokhi *et al.*, 2006), Beijing (Chen *et al.*, 2007), Japan (Khiem *et al.*, 2010), and the United States (Lee *et al.*, 2011). TERI has implemented this integrated modelling framework in India for air pollution source apportionment studies in major metropolitan areas such as Delhi NCR, Ludhiana, Surat, Lucknow, Kanpur, Nashik, Kashipur, Vadodara, Sangareddy, Banaras, and Gurugram.

Brief methodology

The WRF model (version 3.9.1) was performed using ERA5 and 6-hourly ECMWF (European Centre for Medium-Range Weather Forecasts) datasets to generate high-resolution three-dimensional meteorological fields over the grids of the KMC and HMC areas.

Gridded air pollution emission inventory (PM_{10}, $PM_{2.5}$, SO_2, NO_x, CO and NMVOC) at a spatial resolution of 2 km x 2 km (TERI, 2025a,b) was provided as input to the WRF-CMAQ modelling framework to simulate the atmospheric EC concentrations for the year 2023-24.

The boundary conditions of simulations were conducted using a 36 km x 36 km resolution national-scale emission inventory prepared by TERI to account for the inter-regional transport of pollutants to the domain (TERI, 2025a,b).

The ECLIPSE database integrated the international boundary emission inventory into the CMAQ framework (IIASA, 2014).

The long-range atmospheric transport of pollutants originating outside the national boundary was extracted from the Community Atmosphere Model with Chemistry (CAM-Chem) global air quality product developed by the National Center for Atmospheric Research, USA.

The WRF-CMAQ modelling framework (Figure 23) was used to estimate the seasonal atmospheric EC concentrations in the KMC and HMC areas during 2023-24.

In many regions worldwide, the limited availability of BC measurement data has led to the use of EC as a proxy, based on the assumption that the two are interchangeable in both measurement and modelling assessments (Liu *et al.*, 2022, Briggs *et al.*, 2016). However, this assumption introduces inherent uncertainties in estimating radiative forcing and assessing impacts.

To systematically evaluate the relationship between BC and EC and improve its integration into modelling assessments, we analyzed the daily measured BC/EC ratio at each monitoring location. The derived ratio were then applied to estimate BC concentrations from simulated atmospheric EC concentrations, enhancing the accuracy of model-based BC estimations.

Validation of the WRF-CMAQ modelling framework

WRF model simulated wind speed and temperature data during the study period were validated with the data recorded at the Regional Meteorological Centre (RMC), Kolkata. The results yielded R^2 value of approximately 0.7 for wind speed and 0.9 for temperature. Additionally, the observed-to-simulated ratios were about 2.01 for wind speed and 0.95 for temperature. The discrepancies between simulated and observed values can be attributed to several factors, including the RMC data representing point measurements, while the model provides 2 km x 2 km grid value. Again, land-use representation in the WRF model is generalized, which limits its ability to capture localized features, namely buildings and small-scale patterns, that influence surface-level wind speed through increased friction. Despite these limitations, the results demonstrate a strong agreement between simulated and observed meteorological data, offering reliable grounds to use the simulated output in the CMAQ model to estimate atmospheric concentrations in the study domain.

Validation of the modelling framework in the Kolkata Municipal Corporation area

The BC/EC ratio in the KMC area, the seasonal variation in BC/EC ratios across different locations reveals distinct trends influenced by meteorological conditions, emission sources, and atmospheric

processes. The highest BC/EC ratios were estimated in summer, with a mean of 0.616 across all locations. This suggests a greater fraction of optically active BC relative to EC, likely due to enhanced photochemical processing and oxidation in the atmosphere. Higher temperatures and stronger solar radiation can promote secondary aerosol formation and alter the light-absorbing properties of BC, contributing to the increased ratio.

In contrast, the BC/EC ratio is significantly lower during winter, (mean was 0.413 in W1 and 0.353 in W2). This decline can be attributed to an increase in primary emissions from sources such as residential heating, biomass burning, and fossil fuel combustion, which introduce relatively fresh EC with limited atmospheric ageing. Additionally, lower temperatures and more stable atmospheric conditions in winter contribute to pollutant accumulation, reducing oxidation and transformation processes that might otherwise increase the BC fraction.

A slight decrease in the BC/EC ratio from W1 to W2 suggests seasonal shifts in combustion patterns and atmospheric dynamics. Changes in emission sources, such as variations in biomass burning and coal usage, may influence the ratio, along with differences in boundary layer heights, which affect pollutant dispersion. The lower boundary layers in deeper winter can trap pollutants closer to the surface, altering the observed BC/EC balance. Overall, these variations underscore the importance of seasonal influences on BC properties. The higher BC/EC ratios in summer point to increased transformation and ageing of BC, whereas the lower winter values reflect fresher emissions and stagnant atmospheric conditions.

The daily ratio obtained from this assessment was utilized to estimate the BC concentrations from the simulated EC concentrations. The estimated daily BC concentrations with the WRF-CMAQ framework were validated with 24-h BC concentrations measured at different AQM locations during the measurement period (vide Chapter 1). The 1:1 plot (Figure 24) shows that the daily observed and simulated BC concentrations at seven AQM locations in the KMC area were below the 1:1 line. This suggests that the model output exhibited bias, underestimating the overall atmospheric BC

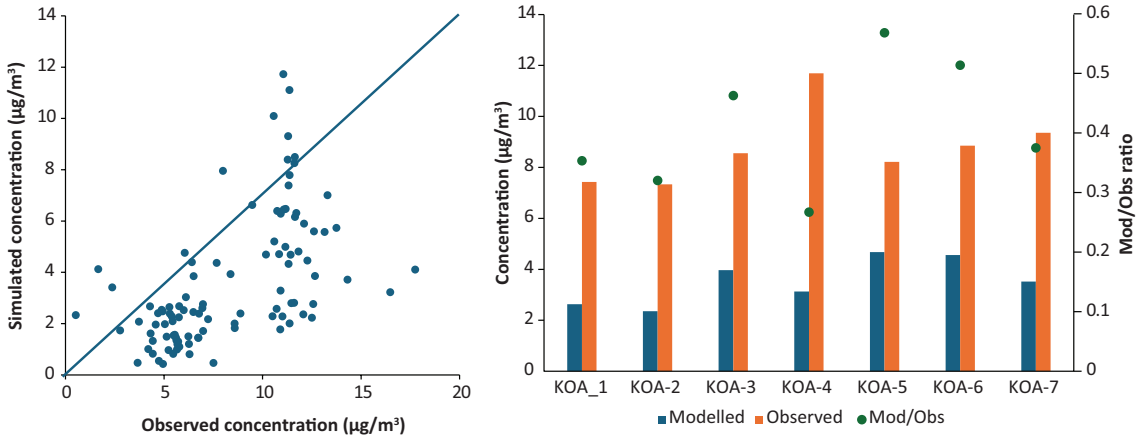

FIGURE 24 1:1 Plot of the simulated and observed BC concentrations and location wise validation of WRF-CMAQ framework in the KMC area

concentrations. The observed-to-simulated BC concentration ratio during the study period in the KMC area was 0.41, indicating a consistent underestimation of BC by the model.

This underestimation is primarily due to the emission inventory. Similar findings have been reported in several studies (Verma *et al.*, 2017; Singh *et al.*, 2021), which found that bottom-up emission inventories for BC can underestimate actual emissions by factors ranging from 3 to 5, compared to observed atmospheric BC concentrations. This suggests that the model validation is reasonable within the context of available datasets and the factors affecting spatial BC concentration estimates.

Additionally, the observed-to-simulated ratio varied between 0.26 and 0.56 at AQM locations within the KMC area. This variation is largely due to the nature of the model's outputs, which represent average concentrations over a 2 km x 2 km grid, while observed values are specific to individual measurement points within that grid. This spatial averaging can lead to discrepancies, particularly in areas with significant local variations in pollutant sources and concentrations, which are often found within urban settings.

Validation of the modelling framework in the Howrah Municipal Corporation area

In the BC/EC ratio monitored in HMC area, the seasonal variation in BC/EC ratios across different locations reveals distinct trends influenced by meteorological conditions, emission sources, and atmospheric processes. The BC/EC ratio fluctuates across W1, summer, and W2, with some locations exhibiting higher values in summer (e.g., HWH_2, HWH_4), while others show an increase in winter 2 (e.g., HWH_1, HWH_3). These variations suggest that local factors, such as emission sources and atmospheric dispersion, play a crucial role in determining BC/EC levels. However, when considering the overall average across all locations, the seasonal differences appear less pronounced, with BC/EC ratios of 0.334 in W1, 0.327 in summer, and 0.317 in W2, indicating a relatively stable trend with only slight seasonal variations.

In some locations, the BC/EC ratio was higher in summer, which could be attributed to enhanced photochemical activity and stronger atmospheric oxidation processes, leading to increased transformation of BC. The higher temperatures and stronger solar radiation during summer promote secondary aerosol formation, which can impact the BC/EC balance. Additionally, greater atmospheric mixing and ventilation in summer can influence the concentration and ageing of the BC.

Conversely, lower BC/EC ratios in winter at certain locations suggest the dominance of fresh emissions of EC-rich particles from biomass burning and vehicle emissions. Winter inversion conditions and lower boundary layer heights often trap pollutants closer to the surface, leading to higher EC concentrations and lower BC/EC ratios. Moreover, seasonal emissions from residential heating and fuel combustion contribute to variations in the ratio.

Differences between W1 and W2 were also evident, with some locations showing a gradual increase in BC/EC ratios while others exhibit a decline. These changes could be linked to shifts in meteorological conditions between early and late winter, including variations in wind patterns, emission intensities, and pollutant accumulation.

Overall, the seasonal variations in BC/EC ratios highlight the complex interplay between meteorology, emission characteristics, and atmospheric processing of BC. The higher BC/EC ratios in summer indicate increased oxidation and photochemical ageing, whereas the lower winter values suggest fresher emissions and stagnant atmospheric conditions. While site-specific differences are evident, the relatively small variations in the overall average BC/EC ratios across seasons suggest a consistent underlying emission pattern.

The daily ratio obtained from this assessment was utilized to estimate the atmopsheric BC concentrations from the simulated atmospheric EC concentrations. The estimated daily BC concentrations were validated with 24-h measured BC concentrations at different AQM locations during the measurement period (vide Chapter 1). The 1:1 plot (Figure 25) shows that the daily observed and simulated BC concentrations at five AQM locations in the HMC area were generally below the 1:1 line. This suggests that the model output, underestimating the overall atmospheric BC concentrations. The observed-to-simulated BC concentration ratio during the study period in the HMC area was 0.63, indicating a consistent underestimation of BC by the model.

The validation analysis of the WRF-CMAQ modelling framework highlights its proficiency in accurately representing the key atmospheric processes that influence atmospheric BC concentrations.

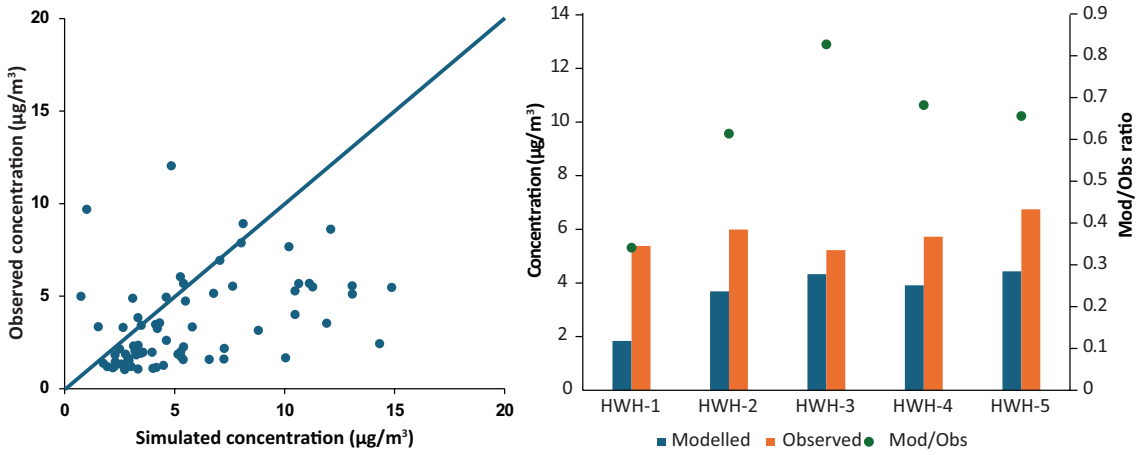

FIGURE 25 1:1 Plot of the simulated and observed BC concentrations and location-wise validation of WRF-CMAQ framework in the HMC area

Simulated spatiotemporal variations in atmospheric concentrations of PM_{10} and $PM_{2.5}$

Kolkata Municipal Corporation area

The spatial variations of estimated atmospheric BC concentrations during the summer and winter seasons of 2023-24 in the KMC area exhibit notable seasonal contrasts (Figure 26) similar to those observed for PM_{10} and $PM_{2.5}$, though the absolute values and contributing processes are distinct given BC's unique sources and atmospheric behaviour.

During the summer season, the simulated BC concentrations across the KMC area were generally lower than that of the winter season (Figure 26). This reduction can be attributed to higher ambient temperatures and enhanced atmospheric mixing, which facilitate the dispersion of BC. In contrast, winter simulations indicate elevated BC levels. The winter season's meteorological conditions—lower temperatures, increased atmospheric stability, and reduced vertical mixing heights—contribute to the accumulation of BC near the surface, thereby leading to higher simulated concentrations.

The simulation results reveal that the highest BC concentrations are predominantly found in the southern, central, and eastern sectors of the KMC area. In particular, industrial activities and dense traffic emissions from adjacent urban and industrial regions, notably areas to the south and east, are likely contributing to the elevated BC levels. Additionally, the reversal in wind patterns between summer and winter plays a key role. In summer, the prevailing southerly winds help to transport relatively cleaner air into the region, whereas the northerly and northwesterly winds in winter align the KMC area with major upwind BC sources, amplifying local concentrations.

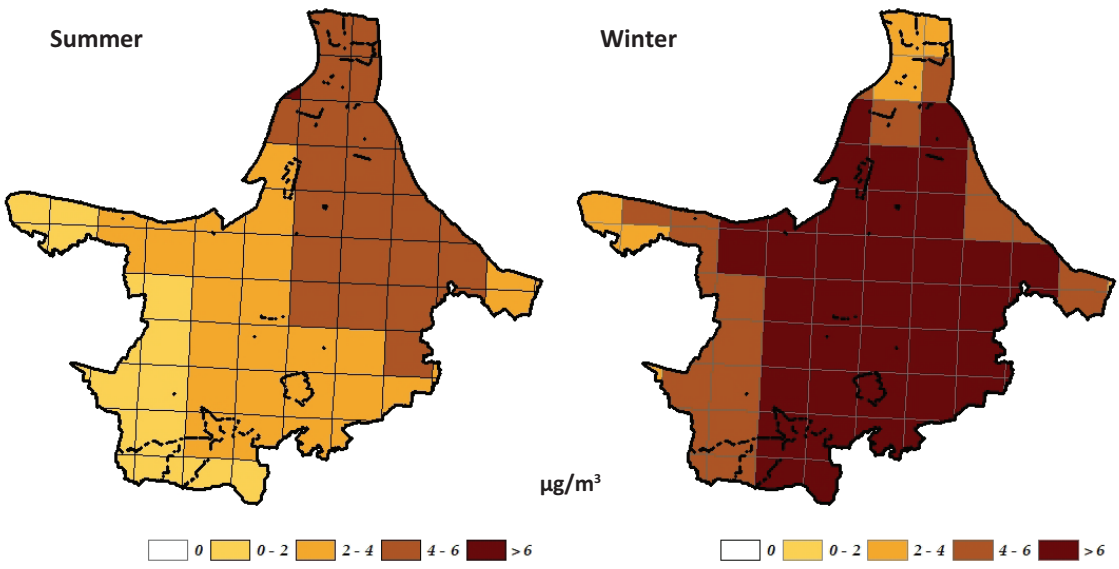

FIGURE 26 Spatial variation of simulated atmospheric BC concentration in the KMC area

Hotspots of BC were primarily observed in regions characterized by high-traffic density and concentrated industrial activities. In the central and southeastern parts of KMC, continuous vehicular emissions, coupled with localized industrial discharges, have been simulated to create persistent BC hotspots. Moreover, areas near major waste disposal sites (similar to those influencing PM concentrations) may also contribute intermittently to higher BC levels, particularly during periods when incineration activities or uncontrolled combustion events occur.

While BC is a marker for combustion-related emissions and serves as a proxy for assessing the impacts of traffic and industrial activities on air quality, the seasonal and spatial variations observed in the simulations underscore the importance of tailored mitigation strategies. The elevated winter concentrations, in particular, highlight the need for targeted interventions during colder months when atmospheric dispersion is limited. In summary, the simulated BC concentrations over the KMC area for the 2023-24 period show marked seasonal differences—with lower levels in summer and higher levels in winter—driven by meteorological factors and directional changes in wind patterns. Spatial patterns indicate that areas with significant upwind contributions, particularly those associated with traffic and industrial emissions, are critical in shaping the distribution of BC. These findings are essential for understanding the dynamics of combustion-related air pollutants in the region and for guiding effective air quality management policies.

Howrah Municipal Corporation area

The spatially distributed simulated concentrations of BC for the summer and winter seasons of 2023-24 in the HMC area indicate that BC concentrations are significantly higher in the winter season due to unfavourable meteorological conditions, which include low-wind speeds and a shallow planetary boundary layer. These factors trap pollutants near the surface, reducing their dispersion and leading to elevated BC levels.

During the summer season, BC concentrations decline as the atmosphere exhibits a greater dispersive capacity. Higher temperatures and increased vertical mixing facilitate pollutant dispersion, preventing BC accumulation near the surface. The prevailing southerly winds originating from the southwestern part of Kolkata introduce relatively cleaner air into the HMC area, as these upwind regions lack major industrial or urban pollution sources. This inflow contributes to improved air quality, with BC levels remaining lower in comparison to winter.

Despite this seasonal improvement, local sources—such as vehicular emissions, industrial activities, and construction—continue to contribute to BC levels in summer. However, their impact is mitigated by the enhanced atmospheric mixing and the cleaner inflow from the south, leading to an overall reduction in concentrations.

In contrast, the winter season brings a shift in wind patterns, with predominant winds arriving from the north and northeast. This shift plays a crucial role in elevating BC concentrations across the HMC area. The stagnant winter atmosphere, characterized by lower temperatures and reduced atmospheric mixing heights, results in poor pollutant dispersion. This leads to BC accumulation in the lower atmosphere, significantly worsening air quality conditions.

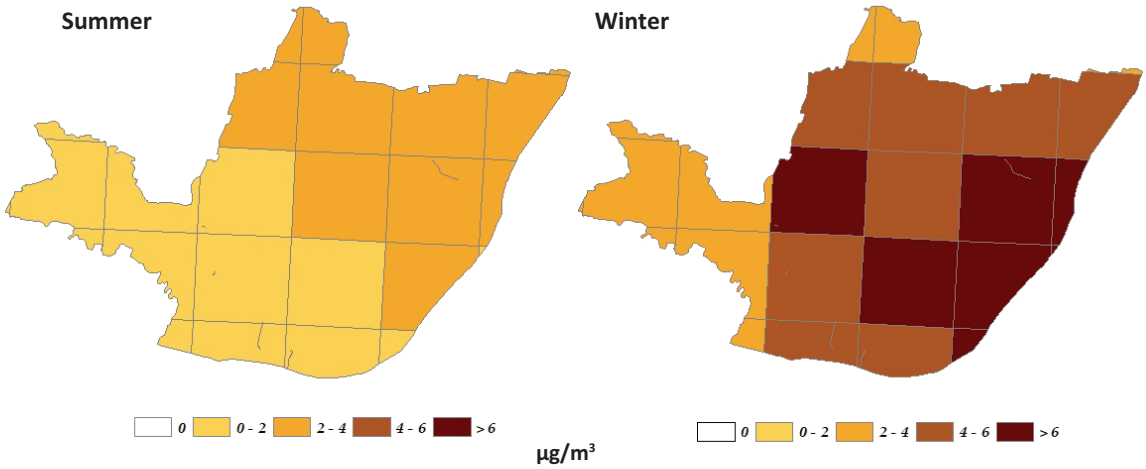

FIGURE 27 Spatial variation of simulated atmospheric BC concentration in the HMC area

Additionally, the northerly and northeasterly winds transport pollutants from upwind industrial and urban areas outside Howrah, further exacerbating BC concentrations in the region. These upwind sources, including emissions from regional industries, traffic, and biomass burning, contribute to the substantial wintertime increase in BC levels.

The simulation results indicate that BC hotspots in the HMC area are closely linked to regions with dense traffic and industrial activity. Areas with high-vehicular movement, particularly near major road networks and transport hubs, exhibit persistently high BC concentrations. Furthermore, industrial zones in and around the HMC area contribute significantly to local BC emissions, reinforcing the seasonal disparity observed in the simulations.

The estimated BC concentrations in the HMC area for the 2023-24 period highlight the strong influence of seasonal meteorology and wind dynamics on air quality. During summer, increased dispersion and southerly wind inflows lead to lower BC concentrations, while in winter, atmospheric stagnation and the influx of pollutants from northern upwind sources cause substantial BC accumulation. These findings underscore the need for targeted air quality management strategies to address seasonal variations in BC pollution and mitigate its impact on public health and the environment.

Limitations of WRF-CMAQ modelling framework

The air pollution source apportionment study using the WRF-CMAQ modelling framework provides valuable insights into the sources and transport of $PM_{2.5}$ and PM_{10} pollutants. However, there are several limitations to consider,

Uncertainties in emissions inventories

The output of the modelling framework is strongly dependent on the quality and precision of the emissions inventories used. In many regions, particularly urban areas in India, these inventories are often incomplete or outdated (this inventory gets outdated almost annually in a dynamic economy like India), leading to uncertainties in estimating pollutant contributions from various sources. For instance, emissions from local industries, vehicles, and agricultural residue burning may be underreported or inaccurately quantified.

In this study, extensive reliance on primary surveys has enabled the collection of multiple datasets which significantly reduced uncertainties associated with emissions data particularly from the study domain.

Simplified representations of atmospheric chemistry

Although CMAQ incorporates advanced atmospheric chemical reactions, it still simplifies these processes to some extent. For example, the secondary formation of particulate matter, such as sulphates and nitrates, may not fully account for the variability in atmospheric conditions or the intricacies of chemical pathways. This limitation arises from gaps in our current understanding of these processes, potentially leading to uncertainties in the modelled concentrations of these species.

Limitations of meteorological data

The WRF model, which supplies meteorological inputs to CMAQ, can occasionally face challenges in accurately capturing local weather patterns, especially in complex metropolitan or mountainous regions. This can impact the simulation of critical factors such as wind patterns, temperature profiles, and pollutant dispersion and transport.

In this study, simulations were conducted at a grid resolution of 2 km × 2 km. While this resolution provides detailed spatial coverage, it inherently averages meteorological data across the entire grid, representing it as a single value for that area. Consequently, the model outputs may differ from monitoring station data, which reflect point-specific measurements within the grid. This discrepancy highlights the limitations of grid-based modelled in capturing fine-scale variations.

Resolution of spatial and temporal scales

While CMAQ can operate across various spatial scales, the resolution of the model may not always capture fine-scale variations in pollutant sources and transport, particularly at the street or neighbourhood level. Similarly, temporal resolution may limit the ability to fully capture short-term pollution events, such as traffic peaks or seasonal agricultural burning that could influence pollutant concentrations.

Limited localized source profiles

Receptor-based models like CMB and PMF benefit from detailed, localized source profiles. CMAQ uses generalized emission profiles, which may not perfectly reflect the specific characteristics of local sources (e.g., vehicle fleet composition, industrial processes, etc.). This can lead to some variations in attributing pollution to particular sources.

Model validation and calibration

Accurate model validation is crucial to assess the reliability of the results. However, the study may have limitations in validating the simulated concentrations with real-world observations due to sparse or inconsistent air quality monitoring networks.

Exclusion of certain source types:

While CMAQ accounts for a wide range of atmospheric processes, some sources of pollution, such as indoor sources or specific micro-scale sources (e.g., small-scale cooking emissions), may not be adequately represented in the model. These sources can contribute to ambient concentrations, especially in urban areas, but might be excluded from the model simulations.

References

Andreae, M. O., & Gelencser, A. (2006). Black carbon or brown carbon? The nature of light-absorbing carbonaceous aerosols. Atmospheric Chemistry and Physics, 6, 3131–3148

Briggs, N. L., & Long, C. M. (2016). Critical review of black carbon and elemental carbon source apportionment in Europe and the United States. Atmospheric Environment, 144, 409-427

Ganguly, D., Ginoux, P., Ramaswamy, V., Winker, D. M., Holben, B. N., and Tripathi, S. N.: Retrieving the composition and concentration of aerosols over the Indo-Gangetic basin using CALIOP and AERONET data, Geophys. Res. Lett., 36, L13806 doi:10.1029/2009GL038315, 2009

Ghosh, S., Verma, S., Kuttippurath, J., & Menut, L. (2020, December). Wintertime Radiative Effects Due to Black Carbon (BC) Over Indo-Gangetic Plain as modelled With Recently Estimated BC Emission Inventories in CHIMERE. In ***AGU Fall Meeting Abstracts*** (Vol. 2020, pp. A112-0003)

Huang, Y., Lu, X., Li, Z., Fung, J. C., Wang, Y., & Chen, Y. (2025). Direct radiative effects of black carbon and brown carbon from Southeast Asia biomass burning with the WRF-CMAQ two-way coupled model. *Environmental Pollution*, *366*, 125425

Huy, L.N., Kim Oanh, N.T., Phuc, N.H., *et al.*, 2021. Survey based inventory for atmospheric emissions from residential combustion in Vietnam. Environ. Sci. Pollut. Res. 28, 10678–10695

Jing, A., Zhu, B., Wang, H., Yu, X., An, J., & Kang, H. (2019). Source apportionment of black carbon in different seasons in the northern suburb of Nanjing, China. Atmospheric Environment, 201, 190-200

Klimont, Z., Cofala, J., Xing, J., Wei, W., Zhang, C., Wang, S., Kejun, J., Bhandari, P., Mathur, R., Purohit, P., Rafaj, P., Amann, M., Chambers, A., and Hao, J.: Projections of SO_2, NO_x and carbonaceous aerosols emissions in Asia, Tellus B, 61, 602–617, doi:10.1111/j.1600-0889.2009.00428.x, 2009

Klimont, Z., Kupiainen, K., Heyes, C., Purohit, P., Cofala, J., Rafaj, P., ... & Schöpp, W. (2017). Global anthropogenic emissions of particulate matter including black carbon. Atmospheric Chemistry and Physics, 17(14), 8681-8723

Kumar, V., Devara, P. C., & Soni, V. K. (2023). Multisite scenarios of black carbon and biomass burning aerosol characteristics in India. ***Aerosol and Air Quality Research***, ***23***(6), 220435

Liu, X., Zheng, M., Liu, Y., Jin, Y., Liu, J., Zhang, B., ... & Yan, C. (2022). Intercomparison of equivalent black carbon (eBC) and elemental carbon (EC) concentrations with three-year continuous measurement in Beijing, China. Environmental Research, 209, 112791

Lu, Z., Q. Zhang, and D. J. Strets. 2011. Sulfur dioxide and primary carbonaceous aerosol emissions in China and India, 1996–2010. Atmospheric Chemistry and Physics 11:9839–64

Lu, Z., Zhang, Q., and Streets, D. G.: Sulfur dioxide and primary carbonaceous aerosol emissions in China and India, 1996–2010, Atmos. Chem. Phys., 11, 9839–9864, doi:10.5194/acp-11-9839- 2011, 2011

Paliwal, U., Sharma, M., & Burkhart, J. F. (2016). Monthly and spatially resolved black carbon emission inventory of India: uncertainty analysis. *Atmospheric chemistry and physics*, ***16***(19), 12457-12476

Pandey, A. and Venkataraman, C.: Estimating emissions from the Indian transport sector with on-road fleet composition and traffic volume, Atmos. Environ., 98, 123–133, doi:10.1016/j.atmosenv.2014.08.039, 2014

Patterson, R. F., & Harley, R. A. (2019). Evaluating near-roadway concentrations of diesel-related air pollution using RLINE. *Atmospheric environment*, *199*, 244-251

Rahimi, S., Liu, X., Zhao, C., Lu, Z., & Lebo, Z. J. (2020). Examining the atmospheric radiative and snow-darkening effects of black carbon and dust across the Rocky Mountains of the United States using WRF-Chem. *Atmospheric Chemistry and Physics*, *20*(18), 10911-10935

Rakshit, G., Saha, P., & Maitra, A. (2023). High black carbon episodes over a polluted metropolis near the land-sea boundary and their impact on associated atmospheric dynamics. Environmental Monitoring and Assessment, 195(2), 256

Rana, A., Dey, S., Rawat, P., Mukherjee, A., Mao, J., Jia, S., ... & Sarkar, S. (2020). Optical properties of aerosol brown carbon (BrC) in the eastern Indo-Gangetic Plain. Science of the Total Environment, 716, 137102

Rana, A., Rawat, P., & Sarkar, S. (2023). Sources, transport pathways and radiative effects of BC aerosol during 2018–2020 at a receptor site in the eastern Indo-Gangetic Plain. Atmospheric Environment, 309, 119900

Sahu, S. K., Beig, G., and Sharma, C.: Decadal growth of black carbon emissions in India, Geophys. Res. Lett., 35, L02807, doi:10.1029/2007GL032333, 2008

Saud, T., R. Gautam, T. K. Mandal, *et al.* 2012. Emission estimates of organic and elemental carbon from household biomass fuel used over the Indo-Gangetic Plain (IGP), India. Atmospheric Environment 61:212–20

Savadkoohi, M., Pandolfi, M., Reche, C., Niemi, J. V., Mooibroek, D., Titos, G., ... & Querol, X. (2023). The variability of mass concentrations and source apportionment analysis of equivalent black carbon across urban Europe. *Environment international*, *178*, 108081

Schultz, M., Backman, L., Balkanski, Y., Bjoerndalsaeter, S., Brand, R., Burrows, J., Dalsoeren, S., de Vasconcelos, M., Grodt mann, B., Hauglustaine, D., Heil, A., Hoelzemann, J., Isaksen, I., Kaurola, J., Knorr, W., Ladstaetter-Weißenmayer, A., Mota, B., Oom, D., Pacyna, J., Panasiuk, D., Pereira, J., Pulles, T., Pyle, J., Rast, S., Richter, A., Savage, N., Schnadt, C., Schulz, M., Spessa, A., Staehelin, J., Sundet, J., Szopa, S., Thonicke, K., van het Bolscher, M., van Noije, T., van Velthoven, P., Vik, A., and Wittrock, F.: REanalysis of the TROpospheric chemical composition over the past 40 years. A long-term global modelling study of tropospheric chemistry funded under the 5th EU framework programme, Final Report, Tech. Rep. 3, Max Planck Institute for Meteorology, Hamburg, 2007

Singh, N., Agarwal, S., Sharma, S., Chatani, S., & Ramanathan, V. (2021). Air pollution over India: causal factors for the high pollution with implications for mitigation. ACS Earth and Space Chemistry, 5(12), 3297-3312

Talukdar, S., Jana, S., & Maitra, A. (2014). Variation of black carbon concentration associated with rain events at a tropical urban location. *Current Science*, 72-78

Talukdar, S., Jana, S., Maitra, A., & Gogoi, M. M. (2015). Characteristics of black carbon concentration at a metropolitan city located near land–ocean boundary in Eastern India. *Atmospheric Research*, ***153***, 526-534

TERI (2025a). Air pollution Emission Inventory, Source Apportionment and atmospheric carrying capacity study of Kolkata West Bengal. West Bengal Pollution Control Board

TERI (2025b). Air pollution Emission Inventory, Source Apportionment and atmospheric carrying capacity study of Howrah city West Bengal. West Bengal Pollution Control Board

US-EPA (2012) Report to Congress on Black Carbon. Department of the Interior, Environment, and Related Agencies. EPA-450/R-12-001.. March 2012

US-EPA [United States Environment Protection Agency] (2022) Gasoline and Diesel Industrial Engines. AP42 Vol I, ChapterIII. https://www3.epa.gov/ttn/chief/ap42/ch03/final/c03s03.pdf

Van den Hove, A., Verwaeren, J., Van den Bossche, J., Theunis, J., & De Baets, B. (2020). Development of a land use regression model for black carbon using mobile monitoring data and its application to pollution-avoiding routing. *Environmental Research*, *183*, 108619

Verma, S., Pani, S. K., & Bhanja, S. N. (2013). Sources and radiative effects of wintertime black carbon aerosols in an urban atmosphere in east India. ***Chemosphere***, ***90***(2), 260-269

Verma, S.; Reddy, D. M.; Ghosh, S.; Kumar, D. B.; Chowdhury, A. K. Estimates of spatially and temporally resolved constrained black carbon emission over the Indian region using a strategic integrated modelling approach. Atmos. Res. 2017, 195, 9–19

Wai, T. H., Apte, J. S., Harris, M. H., Kirchstetter, T. W., Portier, C. J., Preble, C. V., ... & Szpiro, A. A. (2022). Insights from application of a hierarchical spatio-temporal model to an intensive urban black carbon monitoring dataset. *Atmospheric Environment*, *277*, 119069

Zhang, X., Zhu, Z., Cao, F., Tiwari, S., & Chen, B. (2021). Source apportionment of absorption enhancement of black carbon in different environments of China. Science of the Total Environment, 755, 142685

Annexure 1

Attenuation adjustment factors for different EC loadings and wavelength (405 to 980 nm)

EC range (µg/cm²)	ATN_{405}	ATN_{445}	ATN_{532}	ATN_{635}	ATN_{780}	ATN_{808}	ATN_{980}
0–3	1	1	1	1	1	1	1
3–4	1.21	1.19	1.17	1.12	1.13	1.12	1.14
4–5	1.32	1.28	1.25	1.18	1.18	1.18	1.20
5–6	1.42	1.36	1.31	1.23	1.22	1.22	1.24
6–7	1.50	1.43	1.36	1.26	1.25	1.24	1.26
7–8	1.58	1.50	1.43	1.30	1.29	1.29	1.30
8–9	1.64	1.55	1.46	1.33	1.31	1.31	1.33
9–10	1.72	1.62	1.51	1.36	1.33	1.34	1.34
10–11	1.79	1.68	1.57	1.41	1.38	1.38	1.39
11–13	1.88	1.75	1.62	1.45	1.41	1.41	1.42
13–16	2.07	1.91	1.75	1.53	1.49	1.48	1.48
16–20	2.36	2.17	1.99	1.71	1.65	1.66	1.66
20–25	2.71	2.53	2.30	1.97	1.91	1.91	1.93
>25	3.60	3.31	3.07	2.62	2.53	2.53	2.51

Source: Chow et al., 2021

For more information

Project Monitoring Cell
The Energy and Resources Institute (T E R I)
Core 6C, IHC Complex
Lodhi Road
New Delhi – 110 003
India

Tel. 2468 2100 or 2468 2111
E-mail pmc@teri.res.in
Fax 2468 2144 or 2468 2145
Web www.teriin.org
India +91, Delhi (0)11